*Supporting Information for*

# Synthesis of enantiopure $^{18}$F-trifluoromethyl cysteine as a structure-mimetic amino acid tracer for glioma imaging

Shaoyu Liu[1‡], Hui Ma[1‡], Zhanwen Zhang[1,3], Liping Lin[1], Gongjun Yuan[1], Xiaolan Tang[4], Dahong Nie[5], Shende Jiang[6], Guang Yang[2,*] and Ganghua Tang[1,*]

[1]Department of Nuclear Medicine, Guangdong Engineering Research Center for Translational Application of Medical Radiopharmaceuticals, The First Affiliated Hospital, Sun Yat-sen University, Guangzhou 510080, People's Republic of China.
[2]The State Key Laboratory of Medicinal Chemical Biology, College of Pharmacy, Nankai University, Tianjin 300350, People's Republic of China.
[3]Department of Nuclear Medicine, The Sixth Affiliated Hospital, Sun Yat-sen University, Guangzhou 510655, People's Republic of China.
[4]College of Materials and Energy, South China Agricultural University, Guangzhou 510642, People's Republic of China.
[5]Department of Radiation Oncology, The First Affiliated Hospital, Sun Yat-sen University, Guangzhou 510080, People's Republic of China.
[6]School of Pharmaceutical Science and Technology, Tianjin University, Tianjin 300072, People's Republic of China.

‡ These authors contributed equally.
*Corresponding authors: Guang.Yang@nankai.edu.cn; tangghua@mail.sysu.edu.cn.

## Table of Contents

## 1. Material and general methods

All chemical reagents and solvents used in the experiments were obtained from commercial sources without further purification. $K_2CO_3$, Kryptofix 2.2.2 ($K_{2.2.2}$), anhydrous $CH_3CN$ and DMF used for radiosynthesis were purchased from Sigma-Aldrich (Shanghai) Trading Co., Ltd. Sep-Pak light QMA, Sep-Pak Alumina N Plus Light, and Sep-Pak C18 Plus Short cartridges were purchased from Waters (Milford, USA), and Biotechnology grade AG® 11 A8 resin was obtained from Bio-Rad (Hercules, California, USA). Radioactivity was measured by a gamma counter (γ-counter) (SN-6105, Shanghai Nuclear Rihuan Photoelectric Instrument LLC, China). The analytical high-performance liquid chromatography (HPLC) (1260 series, Agilent, USA) and radioactive thin layer chromatography scanner (radio-TLC) (miniGita Star, Raytest, Straubenhardt, Germany) were applied to monitor the reaction extent and analysis of the product purity. The chiral HPLC column (Astec® CHIROBIOTIC® TAG, 25 cm × 4.6 mm, 5 μm) was purchased from Sigma-Aldrich (Shanghai) Trading Co. Ltd. The nuclear magnetic resonance (NMR) spectra including $^{1}H$, $^{13}C$, and $^{19}F$ NMR were recorded on a Bruker 400 MHz or 600 MHz spectrometer. All chemical shifts are reported in ppm relative to tetramethylsilane and peak multiplicities are given as singlet (s), doublet (d), triplet (t), quartet (q), multiplet (m).

## 2. Positron-labelled sulfur-containing amino acid (SAA) tracers

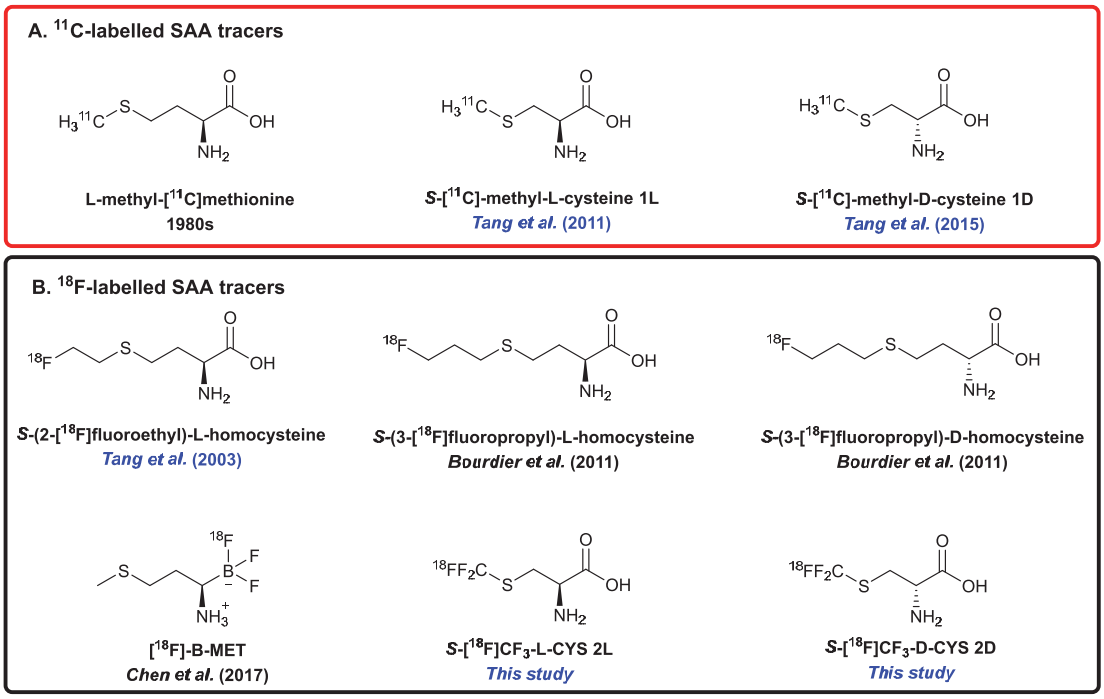


**Figure S1**. Positron-labelled sulfur-containing amino acid (SAA) tracers. **(A)** $^{11}$C-labelled SAA tracers; **(B)** $^{18}$F-labelled SAA tracers.

## 3. Synthetic procedures and spectroscopic data for the compounds

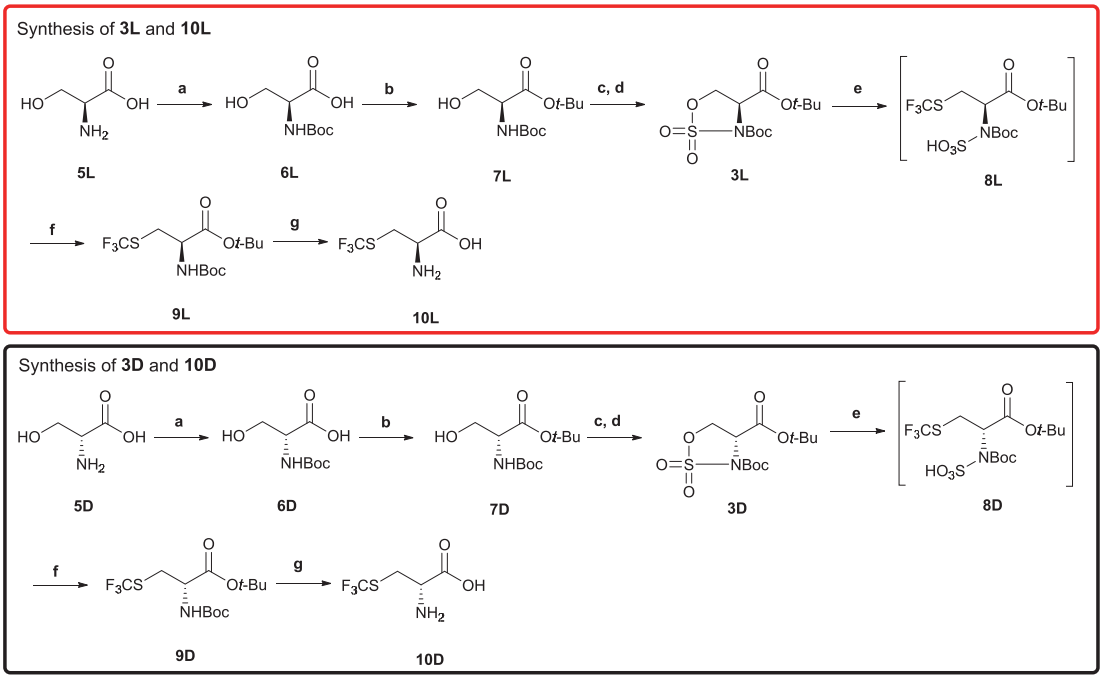

**Scheme S1.** Synthesis of **3L**, **3D**, *S*-$CF_3$-L-CYS **10L**, and *S*-$CF_3$-D-CYS **10D**. Reagents and conditions: a. $(Boc)_2O$, 1M NaOH aq., Dioxane, r.t.; b. 2-*tert*-Butyl-1,3-diisopropylisourea, THF, r.t., 4 h; c. $SOCl_2$, imidazole, $Et_3N$, $CH_2Cl_2$, -20 ºC - r.t., 10 h; d. $NaIO_4$, $RuCl_3 \cdot H_2O$, $CH_3CN$, $H_2O$, 0 ºC, 2 h; e. PDFA, $S_8$, CsF, DMF, 70 ºC, 0.5 h; f. 10 % $NaH_2PO_4$ aq., EtOAc, 50 ºC, 2 h; g. TFA, $CH_2Cl_2$, r.t., 24 h.

As shown in **scheme S1**, firstly, the amino protection reaction of L-serine or D-serine with di-*tert*-butyl carbonate in a mixture of 1M NaOH aq. and dioxane gave compounds **6L,D**.[1] Then the carboxyl group was protected by esterification with 2-*tert*-Butyl-1,3-diisopropylisourea in THF at room temperature to give compounds **7L,D**.[2, 3] Next, the obtained amino β-alcohols were reacted with thionyl chloride in the presence of triethylamine under the catalysis of imidazole to afford the intermediate cyclic-sulfamidites which were subsequently oxidized by sodium periodate with catalytic ruthenium(III) chloride to give cyclic-sulfamidates **3L,D**.[4]

With the desired cyclic-sulfamidates in hand, we immediately set out to investigate whether these compounds were applicable substrates for the exogenous-fluoride-mediated nucleophilic trifluoromethylthiolation reaction. Much to our delight, the ring-opening reaction of these cyclic-sulfamidates **3L,D** proceeded smoothly in the presence of PDFA ($Ph_3P^+CF_2CO_2^-$) and $S_8$ (elemental sulfur) by the addition of external fluoride ion (CsF) under a mild heating condition (70 ºC), leading to the formation of sulfamic acids **8L,D** as the intermediates which were selectively hydrolyzed by a 10% aqueous $NaH_2PO_4$ solution (pH 4.5) in EtOAc (1:1, v/v) to afford **9L,D**. Finally, simultaneous cleavages of the *tert*-butyl and *tert*-butyloxycarboryl protecting groups were carried out

in a mixture of TFA and $CH_2Cl_2$ (3:1, v/v) at room temperature to afford *S*-$CF_3$-L-CYS **10L** and *S*-$CF_3$-D-CYS **10D**.

**1) Potassium 2-bromo-2,2-difluoroacetate**

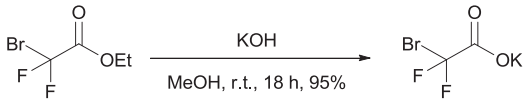


To a solution of potassium hydroxide (2.80 g, 50.00 mmol) in methanol (50 mL) was slowly dropped ethyl 2-bromo-2,2-difluoroacetate (10.25 g, 50.50 mmol) at 0 °C. Afterward, the mixture was naturally warmed to room temperature and stirred for 18 h. The organic solvent was removed, and the residue was further dried under vacuum to obtain a white powder (16.90 g, 95%), which was directly used in the next reaction without further purification.

***Note***: The white powder is easy to absorb moisture.

**2) 2,2-difluoro-2-(triphenylphosphonio)acetate (PDFA)**

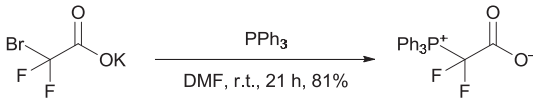


**PDFA**

Triphenylphosphine (12.46 g, 47.50 mmol) was added to a solution of potassium bromodifluoroacetate (16.90 g, 47.50 mmol) in anhydrous DMF (45 mL). The reaction mixture was stirred at room temperature for 21 h. After that, the reaction mixture was filtered with a Buchner funnel, and the residue was thoroughly washed with DMF (3 × 20 mL), $H_2O$ (3 × 20 mL), $Et_2O$ (3 × 20 mL), then dried under reduced pressure to give a white powder (14.04 g, 81%). $^1$H NMR (600 MHz, DMSO-$d_6$) δ 7.95 – 7.91 (m, 2H),

7.83 – 7.75 (m, 9H), 7.65 – 7.54 (m, 1H), 7.41 (dd, $J$ = 10.2, 5.9 Hz, 3H), 7.27 – 7.22 (m, 2H); $^{13}$C NMR (151 MHz, DMSO-$d_6$) δ 136.67, 136.59, 135.33, 135.31, 134.50, 134.43, 133.31, 133.18, 130.29, 130.20, 128.99, 128.80, 128.75, 124.19, 116.45, 115.89; $^{19}$F NMR (565 MHz, DMSO-$d_6$) δ -93.37 (s), -93.55 (s).

**3) (*tert*-butoxycarbonyl)-L-serine 6L**

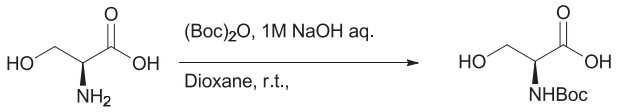


**5L** **6L**

To a solution of L-serine (10.5 g, 100 mmol) in 1M NaOH aq. (200 mL) and dioxane (100 mL) was slowly added ditertbutyldicarbonate (21.8 g, 100 mmol). The mixture was stirred for overnight at room temperature. The reaction solution was washed with diethyl ether (3 × 100 mL). Then the aqueous phase was acidified to pH = 3 with 1N HCl aq., extracted with ethyl acetate (3 × 200 mL). The combined organic phase was washed with water (300 mL), brine (300 mL) and dried over $Na_2SO_4$, then evaporated the solvent to afford a colorless oil (18.46 g, 90%). $[\alpha]_D^{22}$ 6.58 (c 1.0, $CHCl_3$).

**4) *tert*-butyl (tert-butoxycarbonyl)-L-serinate 7L**

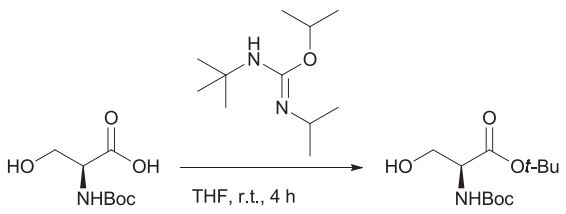


**6L** **7L**

To a solution of (*tert*-butoxycarbonyl)-L-serine (8.20 g, 40 mmol) in anhydrous THF

(100 mL) was slowly added *O*-tert-Butyl-*N, N'*-diisopropylisourea (20.03 g, 100 mmol). Then the mixture was stirred for 4 h at room temperature. The mixture was filtered through Celite® and the organic solvent was evaporated. The residue was purified by flash column chromatography on silica gel (ethyl acetate/petroleum ether 1:5) to give the title compound as a colorless oil which turned to a white solid on standing (6.79 g, 65%). $R_f$ 0.50 (ethyl acetate/petroleum ether 1:2), mp 78-80 °C, $[\alpha]_D^{22}$ +9.73 (c 1.0, $CHCl_3$). $^1H$ NMR (400 MHz, $CDCl_3$) δ 5.42 (s), 4.26 (s), 3.90 (dd, *J* = 6.0, 4.0 Hz), 2.39 (s), 1.49 (s), 1.46 (s). $^{13}C$ NMR (101 MHz, $CDCl_3$) δ 169.95, 156.03, 82.70, 80.22, 64.10, 56.47, 28.42, 28.11.

**5) di-*tert*-butyl (4*S*)-1,2,3-oxathiazolidine-3,4-dicarboxylate 2,2-dioxide 3L**

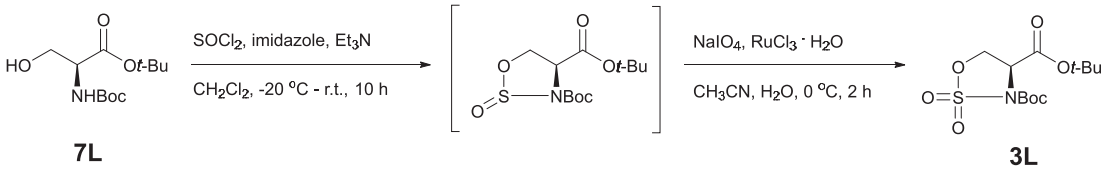


To a solution of imidazole (2.73 g, 40.00 mmol) and triethylamine (3.06 ml, 22.00 mmol) in anhydrous dichloromethane (100 mL) was slowly added thionyl chloride (0.81 mL, 11.00 mmol) during 10 min at about 0 °C. The reaction mixture was stirred at this temperature for 0.5 h and then cooled to -20 °C. A solution of *tert*-butyl (tert-butoxycarbonyl)-L-serinate (2.61 g, 10.00 mmol) in dry dichloromethane (50 mL) was slowly added to the resulting mixture for 30 min. Afterward, the mixture was naturally warmed to room temperature and stirred for 10 h. The reaction mixture was diluted with water (100 mL), extracted with dichloromethane (2 × 100 mL), combined the organic

phase, washed with 10% citrate solution (200 mL), water (200 mL), brine (200 mL), dried over $Na_2SO_4$, and concentrated the solvent to afford the crude cyclic-sulfinamide as a yellow oil which was directly used in the next reaction without further purification.

Ruthenium (III) chloride hydrate (23 mg, 0.11 mmol) and sodium periodate (2.34 g, 11.00 mmol) were added to a solution of the crude cyclic-sulfinamide in a mixture acetonitrile/water (7: 5, 120 ml) at 0 °C. After stirring at 0 °C for 2 h, the mixture was diluted with water (100 mL), extracted with ethyl acetate (3 × 100 mL), combined the organic phase, washed with water (200 mL), brine (200 mL) dried over $Na_2SO_4$, and concentrated the solvent in vacuo. The residue was purified by column chromatography on silica gel (ethyl acetate/petroleum ether 1: 6) to give the title compound (2.59 g, 80%) as a white powder. $R_f$ 0.40 (ethyl acetate/petroleum ether 1:4), mp 115-117 °C; $[\alpha]_D^{22}$ -38.77 (c 0.5, $CHCl_3$). $^1H$ NMR (400 MHz, $CDCl_3$) δ 4.74 (t, *J* = 8.6 Hz, 1H), 4.63 (d, *J* = 8.5 Hz, 2H), 1.56 (s, 9H), 1.51 (s, 9H); $^{13}C$ NMR (101 MHz, $CDCl_3$) δ 166.16, 148.25, 86.00, 84.62, 67.88, 58.27, 28.04, 27.96. MS (EI) Calcd. for $C_{12}H_{21}NO_7S$ $[M+H]^+$: 323.10; found 323.11.

**6) *tert*-butyl N-(*tert*-butoxycarbonyl)-*S*-(trifluoromethyl)-L-cysteinate 9L**

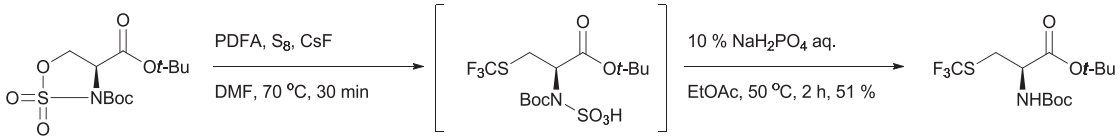


**3L** **8L** **9L**

To a 20 mL sealed tube were added di-*tert*-butyl (4*S*)-1,2,3-oxathiazolidine-3,4-dicarboxylate 2,2-dioxide (194 mg, 0.6 mmol), S8 (115.2 mg, 0.45 mmol), PDFA

(427.6 mg, 1.2 mmol), CsF (455.7 mg, 3.0 mmol) and anhydrous dimethyl formamide (4.5 mL) under inert atmosphere (Ar). The reaction mixture was stirred at 70 ºC for 30 min. After being cooled to room temperature, the solution was transferred to a 100 mL round bottom flask containing a mixture of ethyl acetate (20 mL) and 10% $NaH_2PO_4$ aq. (20 mL) and then stirred at 50 ºC for 2 h. The resulting mixture was taken up with ethyl acetate (80 mL), washed with water (2 × 100 mL), brine (100 mL), dried over $Na_2SO_4$, and concentrated the solvent under vacuum. The resulting solid residue was then washed with cold petroleum ether (20 mL), filtrated and concentrated to obtain the crude product which was purified by short column chromatography (diameter 3 cm × length 6 cm) on silica gel (gradually from petroleum ether to petroleum ether/ethyl acetate 100: 1) to give the title compound (106 mg, 51%) as a yellow oil. $R_f$ 0.3 (ethyl acetate/petroleum ether 30: 1). $[\alpha]_D^{22}$ +18.19 (c 0.5, $CHCl_3$). $^1$H NMR (600 MHz, $CDCl_3$) δ 5.37 (d, *J* = 3.8 Hz), 4.49 (d, *J* = 3.3 Hz), 3.48 (dd, *J* = 9.0, 2.9 Hz), 3.29 (dd, *J* = 9.0, 2.8 Hz), 1.49 (s), 1.45 (s); $^{13}$C NMR (151 MHz, $CDCl_3$) δ 168.72, 155.08, 133.82, 131.79, 129.76, 127.73, 83.67, 80.46, 53.46, 32.31, 29.83, 29.77, 28.36, 28.02; $^{19}$F NMR (565 MHz, $CDCl_3$) δ -40.92 (s). HRMS (EI) Calcd. for $C_{13}H_{22}F_3NO_4S$ $[M+H]^+$: 345.1222; found 345.1219.

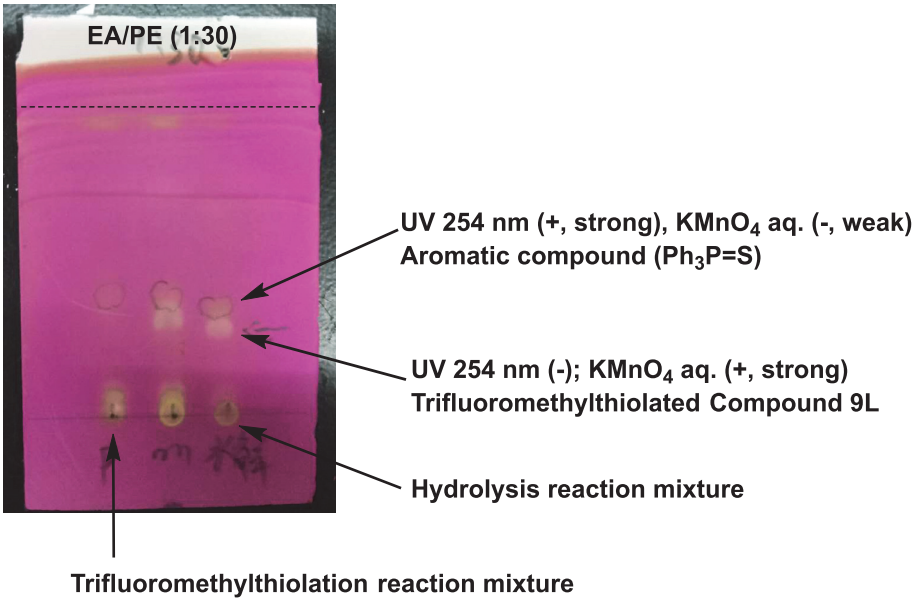


Analysis of hydrolysis reaction mixture by using TLC (ethyl acetate/petroleum ether 1:30 as the developing solvent).

***Note 1:*** To isolate the $CF_3$-product (easily soluble in petroleum ether) from $Ph_3P=S$ (triphenylphosphorus sulfide, slightly soluble in petroleum ether). It is necessary for the crude product to wash with cold petroleum ether.

***Note 2:*** The short column chromatography was gradually eluted from petroleum ether to petroleum ether/ethyl acetate 100: 1. It's necessary to use a large amount of petroleum ether (about 5~6 L) throughout the purification process.

***Note 3:*** Redistilled petroleum ether could effectively decrease the residual solvents (high-boiling point) in the final product.

## 8) *S*-(trifluoromethyl)-L-cysteine 10L

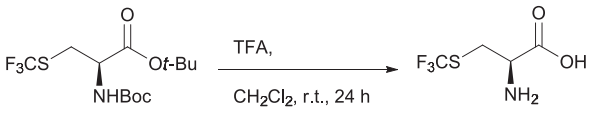


**9L** **10L**

To a solution of *tert*-butyl N-(tert-butoxycarbonyl)-*S*-(trifluoromethyl)-L-cysteinate (69 mg, 0.2 mmol) in anhydrous dichloromethane (1.0 mL) was added Trifluoroacetic

acid (TFA, 3 mL), and the reaction mixture was stirred at room temperature. After stirring for 6 h, the solvent was removed under high vacuum, anhydrous diethyl ether (10 mL) was added to the residue. The crude *S*-$CF_3$-L-CYS was filtered (syringe filter, PTFE, 25 mm diameter, 0.45 μm), then washed with diethyl ether (2 × 10 mL), and finally dissolved with methanol (2 × 10 mL). The organic solvent was concentrated in vacuo to give the title product as a white powder (36 mg, 95%). Mp 232-234 °C; $[\alpha]_D^{22}$ +12.93 (c 0.1, MeOH). $^1$H NMR (600 MHz, $D_2O$) δ 4.04 (dd, *J* = 7.4, 4.4 Hz, 1H), 3.56 (dd, *J* = 15.3, 4.2 Hz, 1H), 3.40 (dd, *J* = 15.2, 7.7 Hz, 1H). $^{13}$C NMR (151 MHz, $CD_3OD$) δ 169.48, 134.92, 132.89, 130.86, 128.84, 53.69, 30.42. $^{19}$F NMR (565 MHz, $CD_3OD$) δ -42.85 (s), -76.55 (s) (trifluoroacetic acid). MS (EI) Calcd. for $C_4H_6F_3NO_2S$ $[M+H]^+$: 189.01; found 189.00.

**Workup of the deprotection reaction by using ethyl ether**

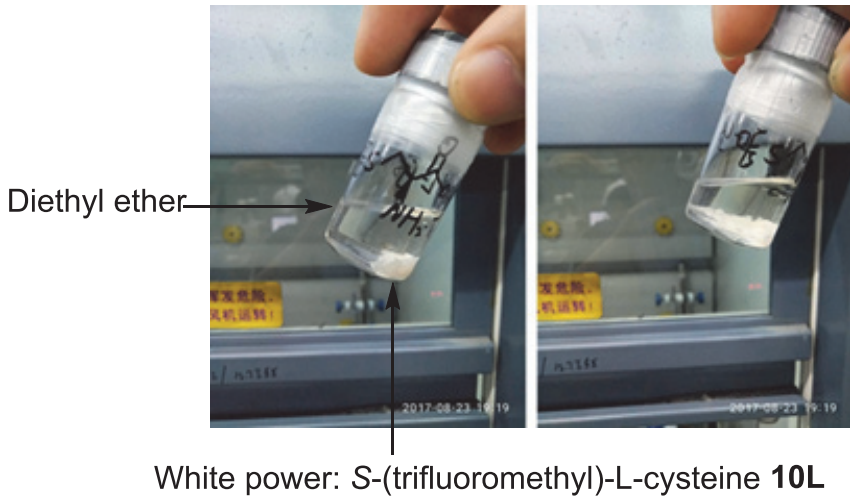


**9) (*tert*-butoxycarbonyl)-D-serine 6D**

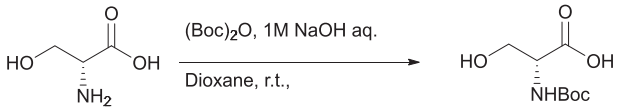


**5D** **6D**

**6D** was synthesized from D-serine as starting material. The synthetic procedure of **D-6** was the same with that of **6L**. White solid, mp 58-60 ºC, $[\alpha]_D^{22}$ -12.75 (c 1.0, $CHCl_3$).

**10) *tert*-butyl (*tert*-butoxycarbonyl)-D-serinate 7D**

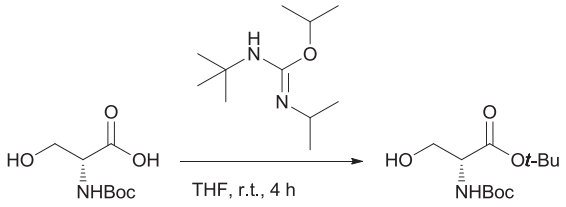


**6D** **7D**

The synthetic procedure of **7D** was the same with that of **7L**. White solid, mp 76-78 ºC, $[\alpha]_D^{22}$ -22.54 (c 1.0, $CHCl_3$). $^1$H NMR (400 MHz, $CDCl_3$) δ 5.43 (s, 1H), 4.26 (s, 1H), 3.90 (d, *J* = 3.6 Hz, 2H), 1.49 (s, 9H), 1.46 (s, 9H). $^{13}$C NMR (101 MHz, $CDCl_3$) δ 170.00, 155.98, 82.51, 80.09, 63.80, 56.40, 28.37, 28.05.

**11) di-*tert*-butyl (*4R*)-1,2,3-oxathiazolidine-3,4-dicarboxylate 2,2-dioxide 3D**

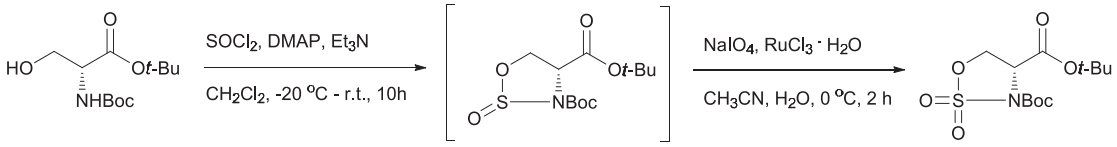


**7D** **3D**

The synthetic procedure of **3D** was the same with that of **3L**. White solid, mp 123-125 ºC, $[\alpha]_D^{22}$ +21.45 (c 1.0, $CHCl_3$). $^1$H NMR (400 MHz, $CDCl_3$) δ 4.76 – 4.71 (m), 4.67 – 4.60 (m), 1.56 (s), 1.51 (s). $^{13}$C NMR (101 MHz, $CDCl_3$) δ 166.13, 148.21, 85.98,

84.60, 67.89, 58.25, 28.01, 27.93. HRMS (EI) Calcd. for $C_{12}H_{21}NO_7S$ $[M+H]^+$: 323.1039; found 323.1037.

**12) *tert*-butyl N-(tert-butoxycarbonyl)-*S*-(trifluoromethyl)-D-cysteinate 9D**

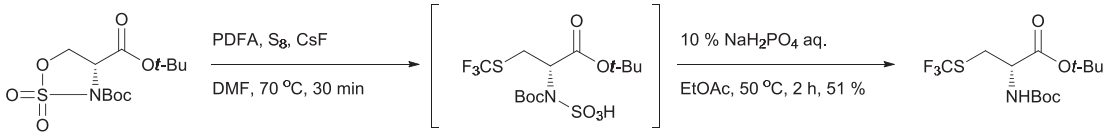


**3D** **8D** **9D**

The synthetic procedure of **9D** was the same with that of **9L**. Yellow oil, $[\alpha]_D^{22}$ -11.15 (c 2.0, $CHCl_3$). $^1$H NMR (600 MHz, $CDCl_3$) δ 5.37 (d, *J* = 3.7 Hz), 4.49 (d, *J* = 2.9 Hz), 3.48 (dd, *J* = 9.0, 2.8 Hz), 3.29 (dd, *J* = 9.0, 2.6 Hz), 1.49 (s), 1.45 (s). $^{13}$C NMR (600 MHz, $CDCl_3$) δ 168.72, 155.10, 133.82, 131.79, 129.76, 127.73, 83.70, 80.52, 53.46, 32.31, 29.84, 29.79, 28.37, 28.02. $^{19}$F NMR (565 MHz, $CDCl_3$) δ -40.94 (s). HRMS (EI) Calcd. for $C_{13}H_{22}F_3NO_4S$ $[M+H]^+$: 345.1222; found 345.1225.

**13) *S*-(trifluoromethyl)-D-cysteine 10D**

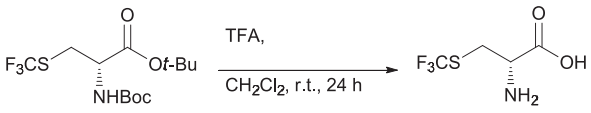


**9D** **10D**

The synthetic procedure of **10D** was the same with that of **10L**. White solid, mp 217-219 °C, $[\alpha]_D^{22}$ -14.01 (c 0.1, MeOH). $^1$H NMR (600 MHz, $D_2O$) δ 4.00 (dd, *J* = 7.4, 4.4 Hz, 1H), 3.55 (dd, *J* = 15.2, 4.3 Hz, 1H), 3.39 (dd, *J* = 15.2, 7.7 Hz, 1H). $^{13}$C NMR (151 MHz, $CD_3OD$) δ 169.86, 135.08, 133.06, 131.03, 129.00, 53.94, 30.63. $^{19}$F NMR (565 MHz, $CD_3OD$) δ -42.85 (S), -76.55 (S) (trifluoroacetic acid). HRMS (EI) Calcd. for

$C_4H_6F_3NO_2S$ $[M+H]^+$: 189.0071; found 189.0067.

## 4. Radiosynthesis of *S*-[$^{18}$F]$CF_3$-L-CYS and *S*-[$^{18}$F]$CF_3$-D-CYS

### 1) Optimization of the reaction conditions ($^{18}$F-trifluoromethylthiolation)

We started our initial research on the $^{18}$F-trifluoromethylthiolation using the conditions reported in the literature.[5] We selected the cyclic-sulfamidate **3L** as a model substrate and used the heating-block-dried $K_{2.2.2}/K^{18}F$ instead of CsF to react with PDFA and $S_8$. However, the intermediate sulfamidite **4L** resulting from the ring-opening $^{18}$F-trifluoromethylthiolation of cyclic-sulfamidates **3L** was obtained in low radiochemical yields (RCY) in 2 minutes, when the reaction was carried out at 70 °C in $CH_3CN$ without additives (**Table S1**, entries 1-2). Subsequent attempts found that the RCY of **4L** increased with the reaction time extending, but no apparent increases beyond 5 minutes (entries 3-4). The use of additives to further optimize the reaction conditions was of no obvious positive impact on the reaction yields (entries 5-7). After that, the investigation of solvent effect indicated that using DMF couldn't give higher RCY (entries 8-9), mainly because the polar intermediate **4L** wasn't easily trapped by the C18 cartridge in the presence of DMF, even if be diluted by water at least 20-fold. Thus, it may not be so helpful to use solvents with a higher polarity in the preparation of **2L** and **2D**. Moreover, we knew that the increase of stoichiometric ratio might be favorable for the improvement of RCY, but this was not optimal because the insoluble substances

would rise accordingly; and as such, we had been committed to exploring this reaction under low stoichiometry conditions.

**Table S1** Optimization of the reaction conditions

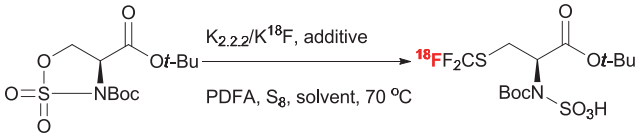


3L 4L

| Entry | additive[a] | Solvent | Time (min) | RCY[b] (%) |
|---|---|---|---|---|
| 1 | Non | $CH_3CN$ | 1 | 6% |
| 2 | Non | $CH_3CN$ | 2 | 10% |
| 3 | Non | $CH_3CN$ | 5 | 23% |
| 4 | Non | $CH_3CN$ | 10 | 26% |
| 5 | CuBr | $CH_3CN$ | 5 | 15% |
| 6 | CuI | $CH_3CN$ | 5 | 20% |
| 7 | TBNI | $CH_3CN$ | 5 | 22% |
| 8 | Non | DMF | 5 | 13% |
| 9 | Non | DMF | 10 | 16% |

[a]Molar ratio of **3L** : PDFA : $S_8$ : additive (1:1:2:1)

[b]RCY of **4L** isolated after Sep-Pak C18 plus short cartridge purification ($n$ = 3)

## 2) Apparatus and Sep Pak cartridges used for the radiosynthesis of 2L and 2D

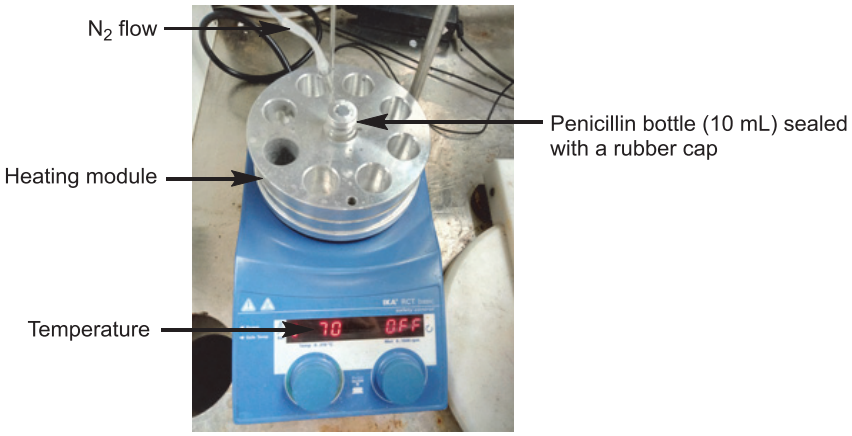


Equipment for the nucleophilic [$^{18}$F]trifluoromethylthiolation reaction

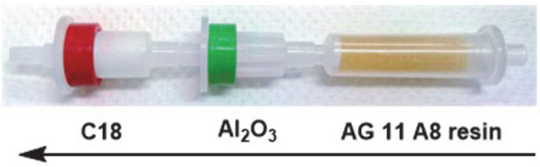


The solid phase extraction (SPE) cartridges used for the final product (**2L** and **2D**) purification

### 3) The nucleophilic $^{18}$F-trifluoromethylthiolation protocol

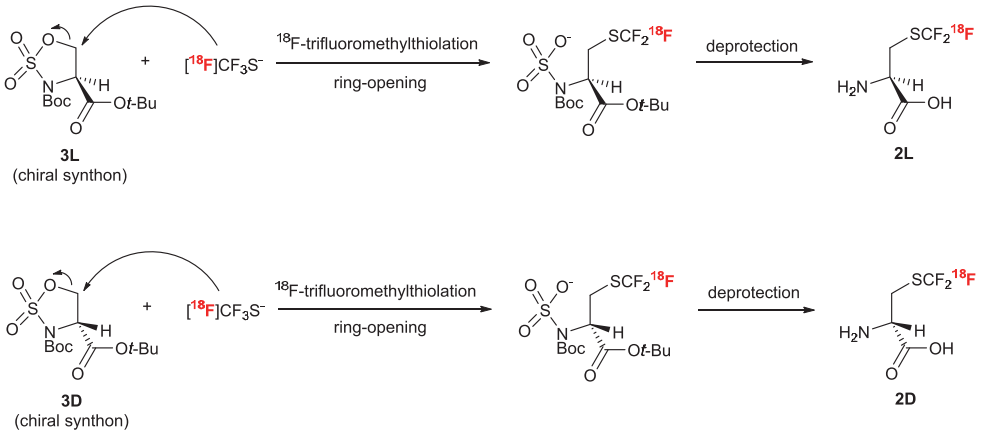


**Scheme S2.** The nucleophilic $^{18}$F-trifluoromethylthiolation protocol for synthesizing enantiopure $^{18}$F-trifluoromethylated cysteines.

As illustrated in **Scheme S2**, serine-derived cyclic sulfamidates (**3L** and **3D**) were used as chiral synthons for the synthesis of $^{18}$F-trifluoromethylated cysteines (**2L** and **2D**).

**2L** and **2D** were synthesized stereoselectively from the serine-derived cyclic sulfamidates **3L** and **3D** *via* a nucleophilic $^{18}$F-trifluoromethylthiolation reaction followed by a deprotection reaction.

### 5. Radio-TLC analysis of the radiochemical purity

The radiochemical purity of *S*-[$^{18}$F]$CF_3$-L-CYS or *S*-[$^{18}$F]$CF_3$-D-CYS was determined by radio-Thin Layer Chromatography (radio-TLC). Radio-TLC was carried out using aluminum sheets pre-coated with silica gel 60 F254 (E. Merck, Germany).

Solvent system: acetonitrile/methanol/water (40:10:10)

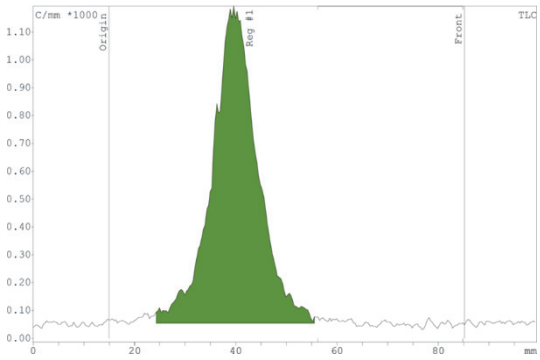


**Figure S2.** Radio-TLC analysis of the radiochemical purity of *S*-[$^{18}$F]$CF_3$-L-CYS **2L** dose

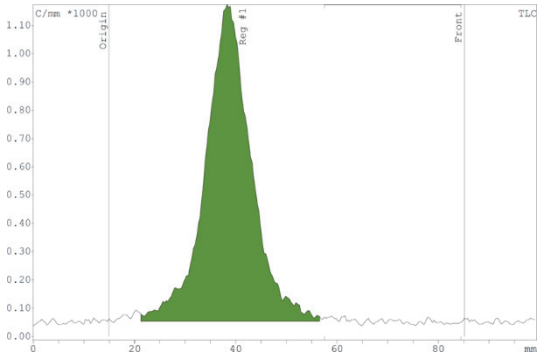


**Figure S3.** Radio-TLC analysis of the radiochemical purity of *S*-[$^{18}$F]$CF_3$-D-CYS **2D** dose

## 6. HPLC analysis of *S*-[$^{18}$F]$CF_3$-L-CYS and *S*-[$^{18}$F]$CF_3$-D-CYS enantiomers

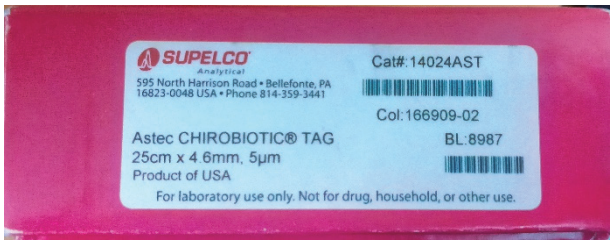


Astec® CHIROBIOTIC® TAG, 25 cm × 4.6 mm, 5 µm

**1)** As shown in the figure below, *S*-[$^{18}$F]$CF_3$-L-CYS ($R_t$ = 7.646 min) and *S*-[$^{18}$F]$CF_3$-D-CYS ($R_t$ = 10.640 min) enantiomers could be well separated, when the pH value of the product solutions was neutralized to pH 7 (AG® 11 A8 Resin-treated). Almost no

racemization was detected. The relative retention times were compared with *S*-$CF_3$-CYS enantiomers (L/D, 4:6) injected under similar conditions to determine *S*-[$^{18}$F]$CF_3$-L-CYS and *S*-[$^{18}$F]$CF_3$-D-CYS, respectively.

| | |
|---|---|
| Apparatus | Agilent 1260 |
| Column | Astec® CHIROBIOTIC® TAG, 25 cm × 4.6 mm, 5 µm |
| Mobile phase | [A] MeOH; [B] $H_2O$ (75:25, A:B) |
| Flow rate | 1 mL/min |
| Sample 1 | 0.4 mg *S*-$CF_3$-L-CYS and 0.6 mg *S*-$CF_3$-D-CYS in 1 mL $H_2O$ |
| Sample 2 | *S*-[$^{18}$F]$CF_3$-L-CYS aq. (pH = 7) |
| Sample 3 | *S*-[$^{18}$F]$CF_3$-D-CYS aq. (pH = 7) |
| Injection | 10 µL |
| Detector 1 | UV, 205 nm (Model 35900E, Agilent, USA) |
| Detector 2 | Radioactive Detector (Model BFC-3200, Bioscan. Inc., USA) |

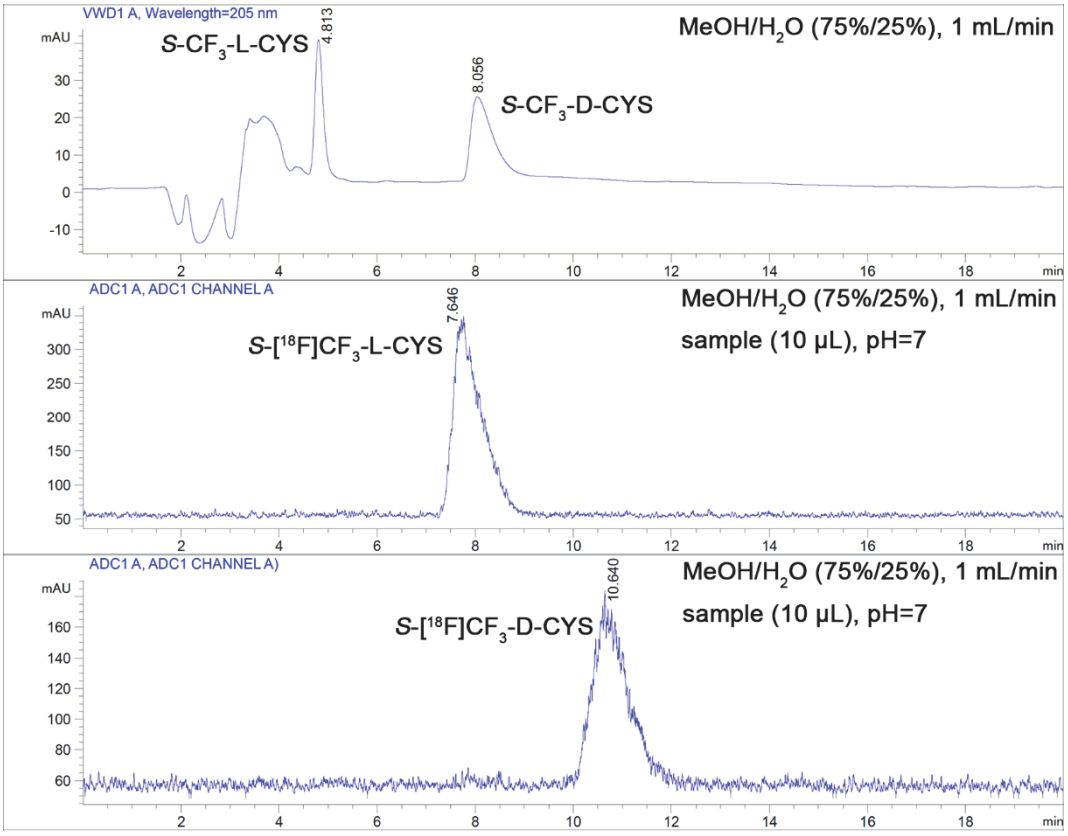


**Figure S4.** Chiral-HPLC analysis of S-[$^{18}$F]$CF_3$-CYS enantiomers

***Note:*** There was a difference in retention times between UV signal and radiation signal due to the distance between the series-connection detectors (UV detector preceding the radiodetector in a line-setting).

2) HPLC analysis of *S*-[$^{18}$F]$CF_3$-CYS enantiomers using the test tube method

To further improve the detection sensitivity (radioactive signal), the test tube method[6] was used for HPLC analysis of *S*-[$^{18}$F]$CF_3$-CYS enantiomers. As shown in the figure below, HPLC samples were collected in 30-second fractions by using the test tube (10 mL) for 20 min. All the samples were counted using a γ-counter for 20 s. The counts were decay-corrected to the initial injection time and added together. The radioactivity counts were expressed as the plotted intensity (cpm) versus fractions to show the profile of the sample. The data were plotted to reconstruct the HPLC spectrum by using Origin® 9 (a complete graphing and data analysis software). The results further confirmed that almost no racemization was detected.

| | |
|---|---|
| Apparatus | Agilent 1260 |
| Column | Astec® CHIROBIOTIC® TAG, 25 cm × 4.6 mm, 5 μm |
| Mobile phase | [A] MeOH; [B] $H_2O$ (75:25, A:B) |
| Flow rate | 1 mL/min |
| Sample 1 | *S*-[$^{18}$F]$CF_3$-L-CYS aq. (pH = 7) |
| Sample 2 | *S*-[$^{18}$F]$CF_3$-D-CYS aq. (pH = 7) |
| Injection | 10 μL |
| Detector | γ-counter (model SN-6105) |

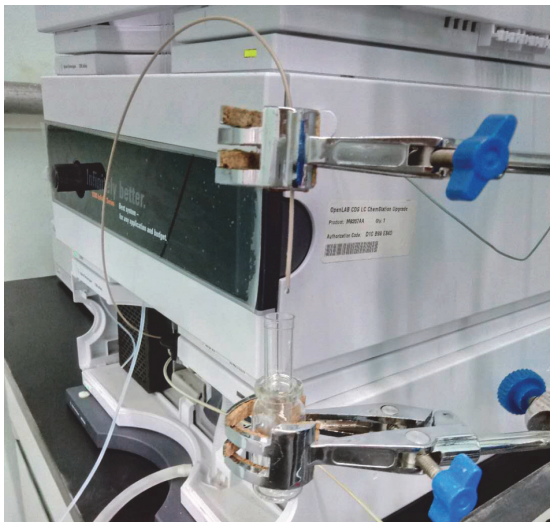

## 7. *In vitro* stability assay

A solution of *S*-[$^{18}$F]$CF_3$-L-CYS or *S*-[$^{18}$F]$CF_3$-D-CYS (2.0 MBq, 20 μL) in sterile saline was added to PBS (pH = 7.4, 200 μL) and was incubated at 37 °C for 2 h. S-[$^{18}$F]$CF_3$-L-CYS and S-[$^{18}$F]$CF_3$-D-CYS exhibited good stability in PBS, as determined by chiral-HPLC analysis. Almost no racemization was found, and the intact tracer was more than 95%.

| | |
|---|---|
| Apparatus | Agilent 1260 |
| Column | Astec® CHIROBIOTIC® TAG, 25 cm × 4.6 mm, 5 μm |
| Mobile phase | [A] MeOH; [B] $H_2O$ (75:25, A:B) |
| Flow rate | 1 mL/min |
| Sample 1 | *S*-[$^{18}$F]$CF_3$-L-CYS in PBS |
| Sample 2 | *S*-[$^{18}$F]$CF_3$-D-CYS in PBS |
| Injection | 20 μL |
| Detector | Radioactive Detector (Model BFC-3200, Bioscan. Inc., USA) |

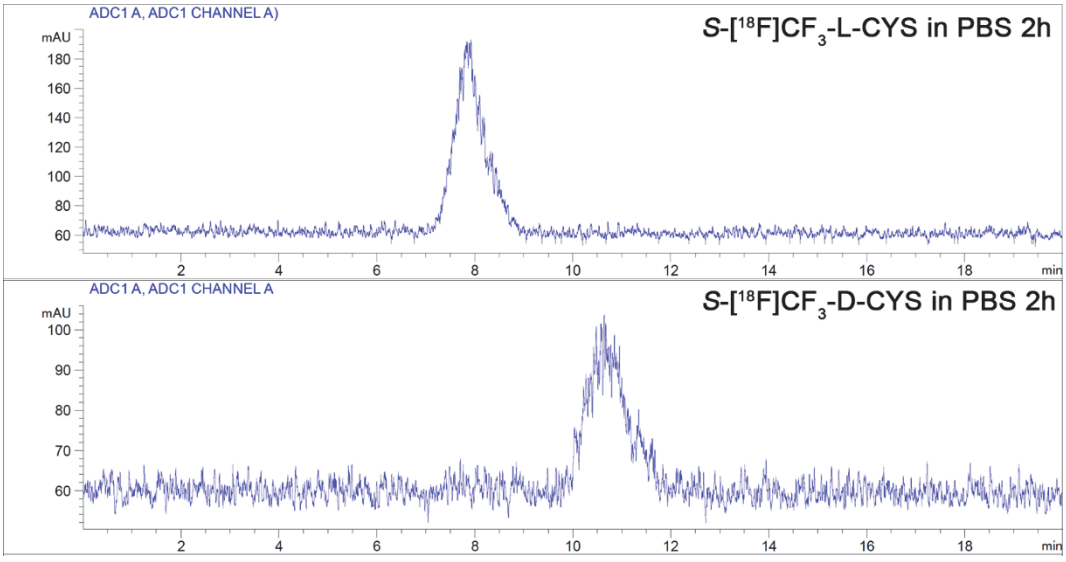


**Figure S5.** HPLC analysis of the stability of S-[$^{18}$F]$CF_3$-CYS enantiomers in PBS

**8. Determination of partition coefficients (logP)**

The partition coefficients for each enantiomers (**2L** or **2D**) were determined by adding radiotracer solution (20 μL, 5 μCi; 0.19 MBq) to an equal volume (*n*-octanol/water; 5 mL/5 mL) mixture. The mixture was vortexed vigorously for 5 min and then centrifuged at 3000 rpm for 15 min. Aliquot of 300 μL *n*-octanol or 300 μL water was taken out from each phase, then respectively counted by the γ-counter, taking care to avoid cross-contamination and interaction effect between two phases. The partition coefficients were calculated according to the formula: logP = $\log_{10}$ (counts of *n*-octanol/counts of water) and reported by averaging nine measurements.

**9. Cell culture**

The C6 glioma cell line was kindly provided by the Cell Bank of the Chinese Academy of Sciences in Shanghai. All cells were cultured in Dulbecco's modified Eagle's medium (DMEM, GIBCO) supplemented with 10% fetal bovine serum (FBS, GIBCO), 1% 100 μg/ml streptomycin and 100 IU/ml penicillin (MRC) at 37 °C in the humidified circumstance containing 5% $CO_2$. When cells reached 90% confluence in the logarithmic growth phase, they were harvested or passaged.

**10. C6 tumor-bearing mice models**

*All the animal experiments were approved by the Committee on the Ethics of Animal Experiments of the First Affiliated Hospital, Sun Yat-sen University and performed*

*strictly according to the Guide for the Care and Use of Laboratory Animals of the Ministry of Science and Technology of the People's Republic of China.*

Four- to six-week-old male nude mice of BALB/c origin were purchased from Beijing Vital River Laboratory Animal Technology Co., Ltd. To establish C6 tumor models, they were subcutaneously implanted $5 \times 10^6$ C6 cells in 0.1 ml of PBS into the right shoulder flanks. When the tumor size reached 0.6-1.0 cm in diameter (about 2-3 weeks after inoculation), animals were subjected to studies.

**11. Turpentine-induced inflammation**

Eight Kunming mice (6–8 weeks old, 25–30 g weight) were used to induce aseptic inflammatory models. Turpentine (0.2 mL) was injected intramuscularly into the thigh of the left hind leg. The mass of the inflammatory tissue grew to 10–15 mm on the 4th day after inoculation of turpentine oil. The mice were randomly assigned to two groups and were anesthetized with 2% pentobarbital (35 mg/Kg). Then, the mice were intravenously administered 0.74 MBq (20 μCi) [$^{18}$F]FDG or **2D** through the tail vein, respectively. Sixty minutes post-injection, the mice were sacrificed by cervical dislocation. The organs of interest (blood, brain, inflammatory muscle and normal muscle) were rapidly dissected and weighed, then the radioactivity was counted with a γ-counter. All measurements were background-subtracted and decay-corrected to the time of injection, and the values were expressed as percent of injected dose per gram

of wet tissue (% ID/g). The uptake ratios of inflammation-to-muscle, and inflammation-to-blood were also calculated.

**Table S2.** Uptake of [$^{18}$F]FDG and *S*-[$^{18}$F]$CF_3$-D-CYS **2D** in mice model of inflammation.

| Parameter | [$^{18}$F]FDG | *S*-[$^{18}$F]$CF_3$-D-CYS |
|---|---|---|
| Brain | 4.37 ± 0.25 | 0.91±0.08 |
| Inflammation | 6.93 ± 0.90 | 1.63 ± 0.11 |
| Muscle | 0.95 ± 0.07 | 1.32 ± 0.17 |
| Blood | 1.02 ± 0.15 | 1.44 ± 0.24 |
| Inflammation-to-muscle ratio | 7.25 ± 0.67 | 1.25 ± 0.16 |
| Inflammation-to-Blood ratio | 6.82 ± 0.74 | 1.15 ± 0.16 |

Data (organ uptake) are expressed as average %ID/g ± SD ($n$ = 4, 60 min post-injection).

## 12. Time-dependent cell uptake assay

C6 cells at a density of $1\times10^5$ cells/well were seeded into 24-well plates and incubated at 37 ºC for overnight. After washing with warm phosphate-buffered saline (PBS), the cells were incubated with *S*-[$^{18}$F]$CF_3$-L-CYS **2L** or *S*-[$^{18}$F]$CF_3$-D-CYS **2D** (0.187 MBq; 5 μCi in 200 μl of PBS) at 37 ºC for 5, 10, 20, 30, 60, 90 and 120 min. The cells were washed three times with cold PBS, lysed by 0.5 mL of 0.5 M NaOH aq., collected into test tubes and measured by a γ-counter (SN-6105). The protein content was calculated by the method of the bicinchoninic acid (BCA) assay. Cell uptake was expressed as the percentage of the injected dose per 100 microgram of protein (%ID/100 μg protein). Experiments were performed three times with quadruplicate wells.

## 13. Competitive cell uptake assay

C6 cells at a density of $1\times10^5$ cells/well were seeded into 24-well plates 24 h prior to experiments, which were repeated three times with quadruplicate wells for each group.

The inhibition experiments were performed with 137 mmol/L NaCl medium or Choline Chloride medium in sterile water for incubation to induce the condition with or without the presence of $Na^+$ ($+Na^+$ or $-Na^+$). The solution in $+Na^+$ or $-Na^+$ medium was at a concentration of 15 mmol/L inhibitors or *S*-methyl-L-cysteine (L-MCY), such as α-(methylamino)isobutyric acid (MeAIB) targeting at system A, serine (Ser) system ASC, 2-amino-2-norbornane-carboxylic acid (BCH) system $B^{0+}$ in $+Na^+$ condition and L in $-Na^+$ condition.

After washing with warm $+Na^+$ or $-Na^+$ medium, cells were incubated with 200 μL of *S*-[$^{18}$F]$CF_3$-L-CYS **2L** or *S*-[$^{18}$F]$CF_3$-D-CYS **2L** (0.187 MBq; 5 μCi in $+Na^+$ or $-Na^+$ medium) at 37 °C for 15 min, with co-incubation of 200 μL of each inhibitor or 200 μL of pure NaCl medium or Choline Chloride medium for control. The cells were washed three times with cold PBS, lysed by 0.5 mL of 0.5 M NaOH aq., collected into test tubes and measured by a γ-counter. The results of each well are normalized by the equation: the uptake data (expressed as a percentage of the injected dose per 100 microgramm of protein, % ID/100 μg protein) = (the final measured radioactivity/the decay-corrected radioactivity originally added)/protein content. And the final uptake values of every group were averaged and expressed as the percentage of the uptake of the $Na^+$-containing control group, which was supposed to be 100%.

**14. Protein incorporation assay**

C6 cells at a density of $2\times10^6$ cells/well were seeded into 6-well plates 24 h before experiments. After washing with warm PBS, cells per well were added 400 μL of *S*-[$^{18}$F]$CF_3$-L-CYS **2L** or *S*-[$^{18}$F]$CF_3$-D-CYS **2D** (0.925 MBq; 25 μCi in PBS) and incubated at 37 ºC for 30 and 120 min. The cells were washed three times with cold PBS, separated by 0.5 ml of 0.25% trypsin, and resuspended in PBS. The samples were centrifuged (13,000 rpm, 5 min), the supernatant removed, and the cells suspended in 200 μL of 1% Triton-X 100. After vortex mixing, the samples were added 0.5 mL of 20% trichloroacetic acid (TCA), and put into ice for 10 min. After that, the samples were centrifuged (13000 rpm, 15 min) and the supernatant was collected into test tubes. The TCA-precipitate was washed by PBS and centrifuged for three cycles. Every time the supernatant was collected into corresponding test tubes mentioned above. The pellets were re-suspended in PBS and transferred into new test tubes. The radioactivity in TCA-solution fraction or TCA-precipitation was measured by a gamma counter. Protein incorporation was reported as the percentage of TCA-perceptible activity. Experiments were performed twice times with triplicate wells.

**15. Biodistribution studies by dissection**

Normal healthy Kunming mice were used instead of tumor-bearing mice to reduce the costs and numbers of animal models used in the biodistribution study. Mice (6–8 weeks old, 25–30 g weight) were injected with 0.74 MBq (20 μCi) of **2L** or **2D** in 100 μL of saline via the tail vein, respectively. The groups of mice (four mice per group at each

time point) were sacrificed by cervical dislocation at various times (5, 30, 60 and 90 min after injection of **2L** and **2D**). The organs of interest (blood, brain, heart, lung, liver, spleen, pancreas, kidney, stomach, intestine, bone and muscle) were rapidly dissected and weighed, and the radioactivity was counted with a γ-counter. All measurements were background-subtracted and decay-corrected to the time of injection, and the values were expressed as percent of injected dose per gram of wet tissue (% ID/g).

**16. Small-animal PET imaging studies**

*In vivo* PET/CT imaging was conducted by the Inveon small-animal PET/CT scanner (Siemens, Germany) equipped with the Inveon Research Workplace 4.1 software.

**1)** *The static micro-PET imaging studies* were conducted with 3.7 MBq of **2D** (injection *via* the tail vein) on the C6 tumor-bearing BALB/c mice ($n$ = 3) at 45, 60, 75 min post-injection. All mice (male) were kept fasting for 4 h and were anesthetized with 2% pentobarbital (35 mg/Kg) *before the imaging experiments*.

**2)** *The static micro-PET imaging studies* were conducted with 3.7 MBq of [$^{18}$F]FDG (injection *via* the tail vein) on the same C6 tumor-bearing BALB/c mice ($n$ = 3) at 60 min post-injection. The mice (male) were kept fasting for 4 h and were anesthetized with 2% pentobarbital (35 mg/Kg) *before the injection of [$^{18}$F]FDG*.

**3)** *The dynamic micro-PET imaging studies* were conducted with 3.7 MBq of **2D** (injection *via* the tail vein) on other C6 tumor-bearing BALB/c mice ($n$ = 3) over a

period of 90 min (dynamic, 5 min/frame). All mice (male) were kept fasting for 4 h and were anesthetized with 2% pentobarbital (35 mg/Kg) *before the injection of* ***2D***.

The images were reconstructed, and regions of interest (ROIs) were drawn over the tumor and organs on decay-corrected whole-body coronal images using vendor software (Iveon Research Workplace). The radioactivity in each volume of interest was obtained from mean pixel values, which were converted to MBq/mL using a conversion factor. Assuming a tissue density of 1 g/mL, the ROIs were converted to MBq/g and then divided by the administered activity to obtain an imaging ROI-derived %ID/g.

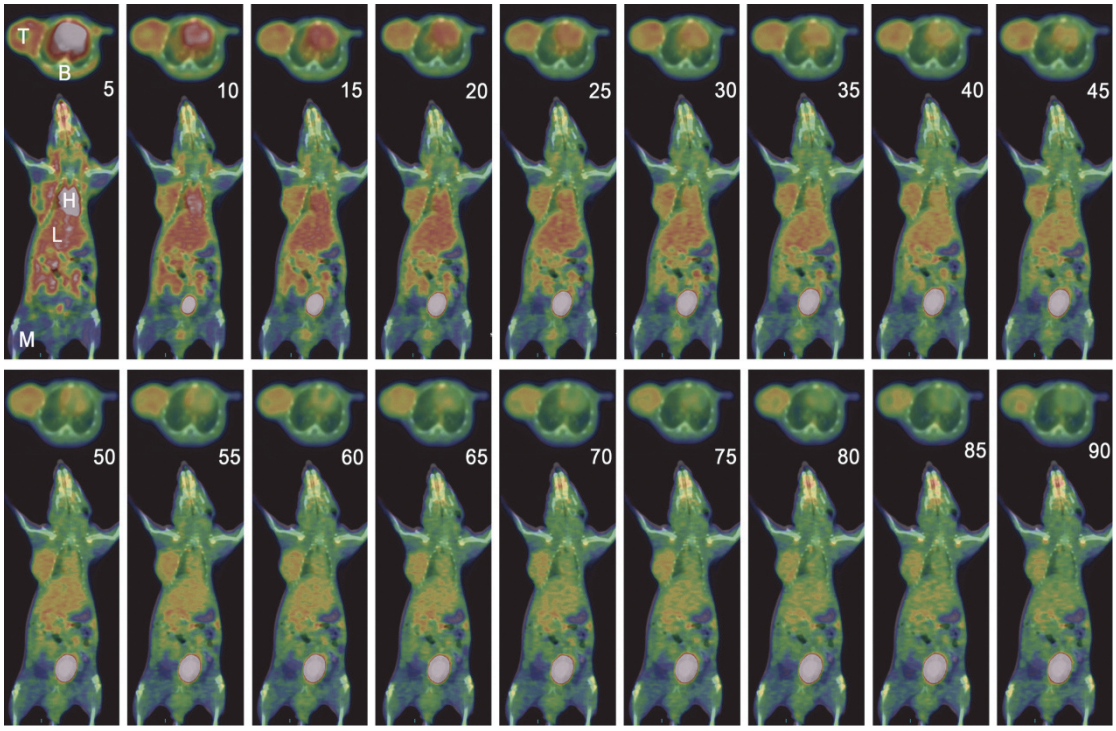


**Figure S6.** Dynamic micro-PET images of C6 glioma-bearing mice scanned after injection of S-[$^{18}$F]$CF_3$-D-CYS **2D** (from 0 to 90 min).

***Note:*** Although no systematic studies were performed, pentobarbital might interfere with the distribution patterns of **2D** by slowing down the excretion of the tracer from the liver.

**17. H&E staining of subcutaneous-induced C6 tumor in BALB/c nude mice**

Mice were sacrificed by mercy killing. C6 tumor tissues were removed, fixed in 4% paraformaldehyde, and embedded in paraffin for hematoxylin and eosin (H&E) staining. Subsequently, samples were observed under an optical microscopy.

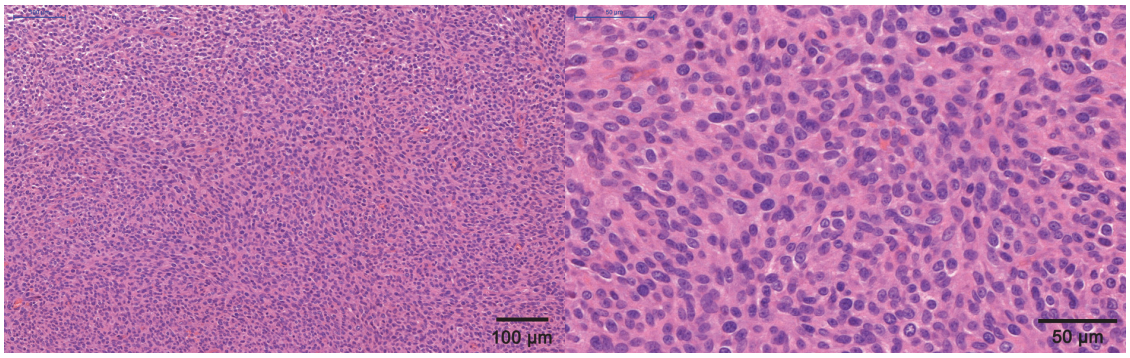


**18. H&E staining of turpentine-induced inflammation in Kunming mice**

Mice were sacrificed by mercy killing. Inflammatory tissues and normal striated muscle tissues were removed, fixed in 4% paraformaldehyde, and embedded in paraffin for hematoxylin and eosin (H&E) staining. Subsequently, samples were observed under an optical microscopy.

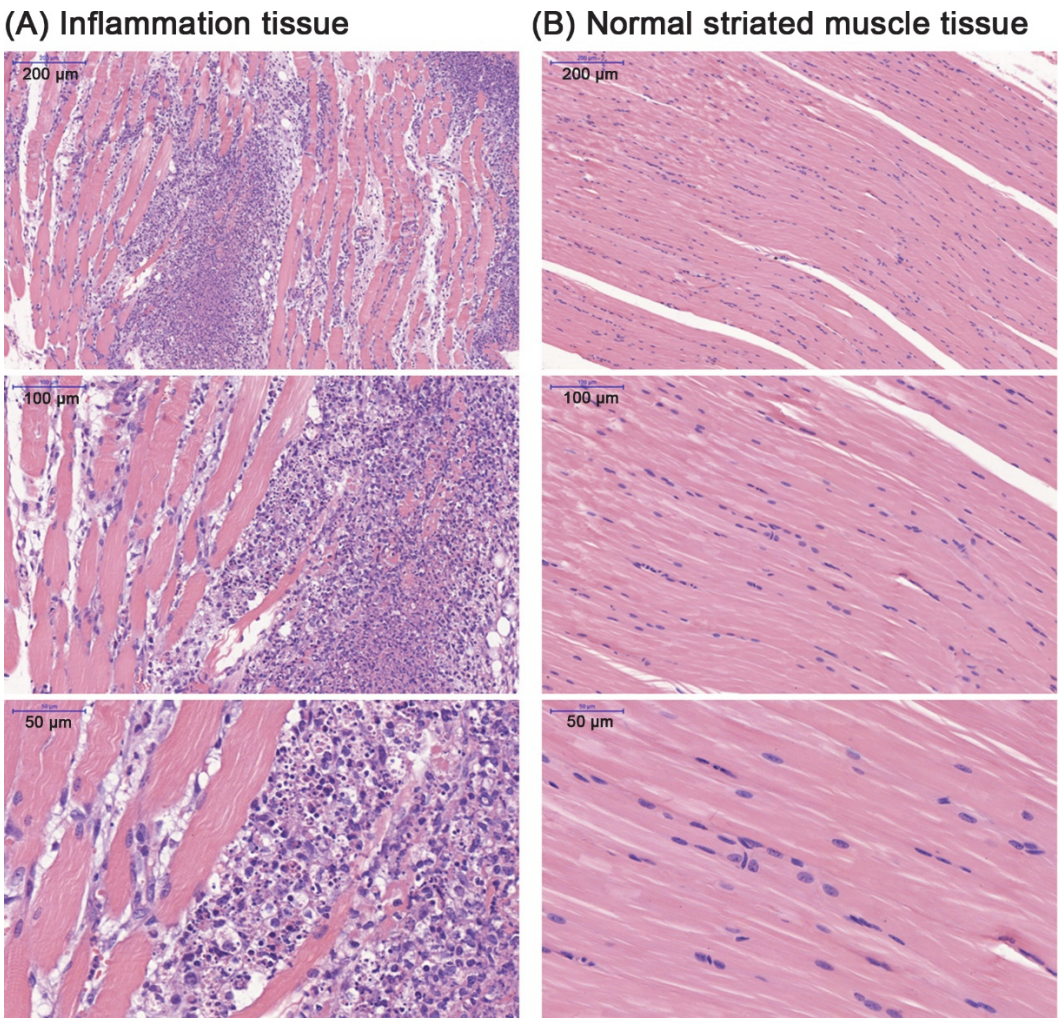


## 19. References

1. Pave G, Usse-Versluys S, Viaud-Massuard MC, Guillaumet G. Synthesis of 3-aminochroman derivatives by radical cyclization. Org lett. 2003; 5: 4253-6.
2. Ducrot P-H, Allais F, Martinet S. Straightforward Total Synthesis of 2-O-Feruloyl-l-malate, 2-O-Sinapoyl-l-malate and 2-O-5-Hydroxyferuloyl-l-malate. Synthesis. 2009; 2009: 3571-8.
3. Cambeiro XC, Martin-Rapun R, Miranda PO, Sayalero S, Alza E, Llanes P, et al. Continuous-flow enantioselective alpha-aminoxylation of aldehydes catalyzed by a polystyrene-immobilized hydroxyproline. Beilstein J Org Chem. 2011; 7: 1486-93.
4. McConathy J, Martarello L, Malveaux EJ, Camp VM, Simpson NE, Simpson CP, et al. Radiolabeled Amino Acids for Tumor Imaging with PET: Radiosynthesis and Biological Evaluation of 2-Amino-3-[$^{18}$F]fluoro-2-methylpropanoic Acid and 3-[$^{18}$F]Fluoro-2-methyl-2-(methylamino)propanoic Acid. J Med Chem. 2002; 45: 2240-9.
5. Zheng JL, Wang L, Lin JH, Xiao JC, Liang SH. Difluorocarbene-Derived Trifluoromethylthiolation and [$^{18}$F]Trifluoromethylthiolation of Aliphatic Electrophiles. Angew Chem. 2015; 54: 13236-40.
6. Lieberman BP, Ploessl K, Wang L, Qu WC, Zha ZH, Wise DR, et al. PET imaging of glutaminolysis in tumors by (2S,4R)-4-[$^{18}$F]fluoroglutamine. J Nucl Med. 2011; 52: 1947-55.

## 20. $^{1}H$, $^{13}C$ and $^{19}F$ NMR spectra for the compounds

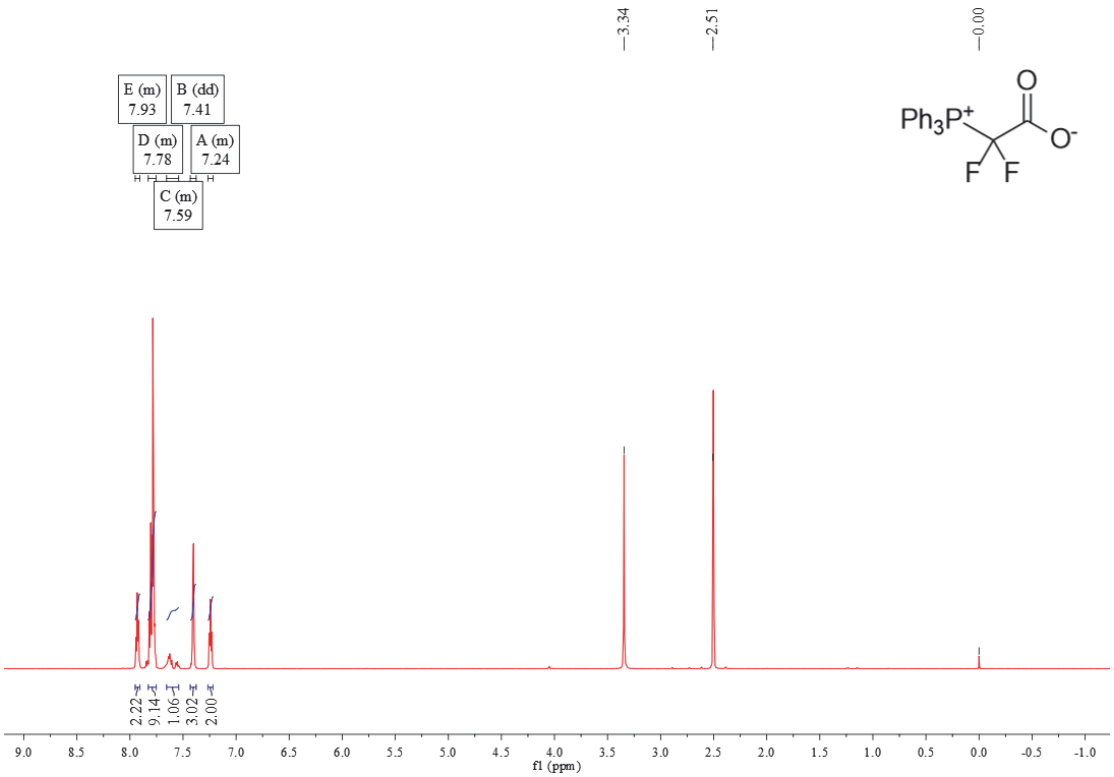


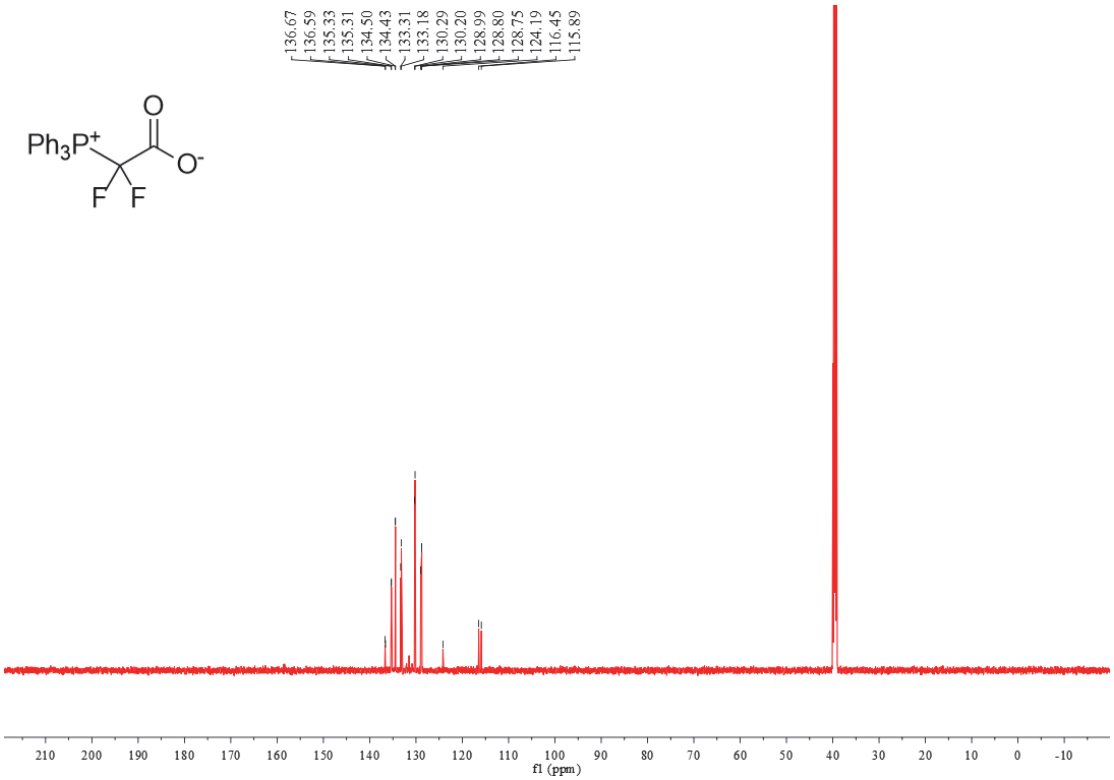

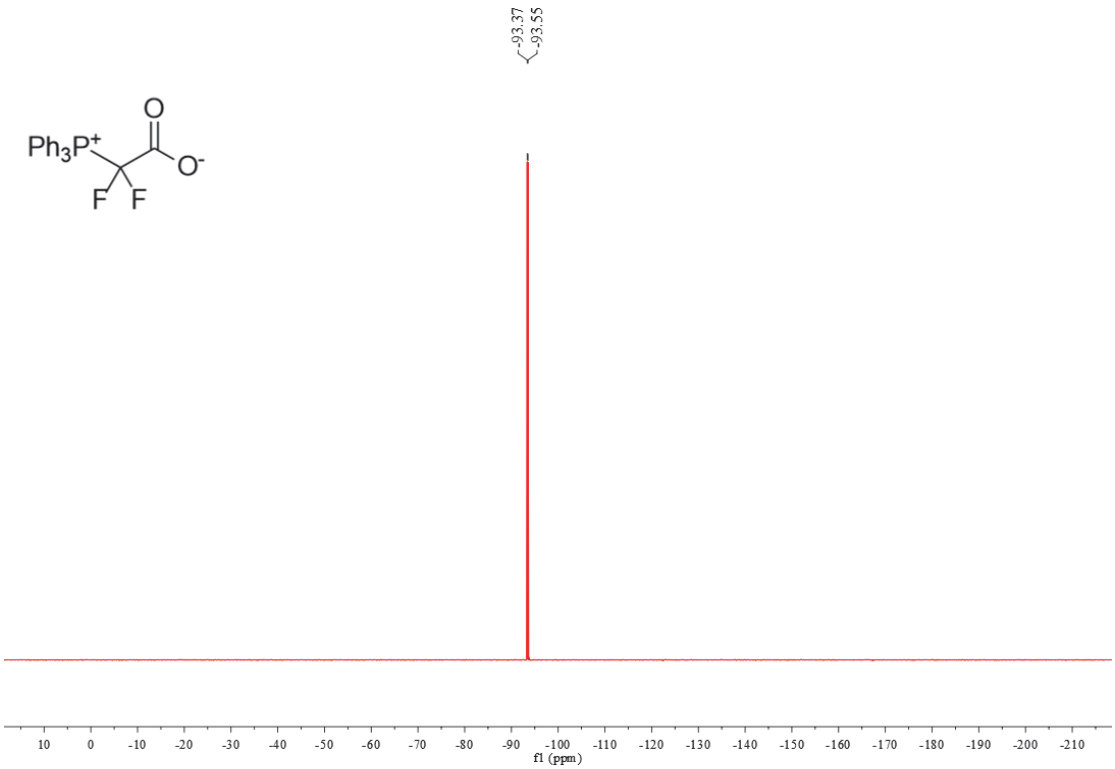
-93.37
-93.55
Ph3P+
O
O-
F F
10 0 -10 -20 -30 -40 -50 -60 -70 -80 -90 -100 -110 -120 -130 -140 -150 -160 -170 -180 -190 -200 -210
f1 (ppm)

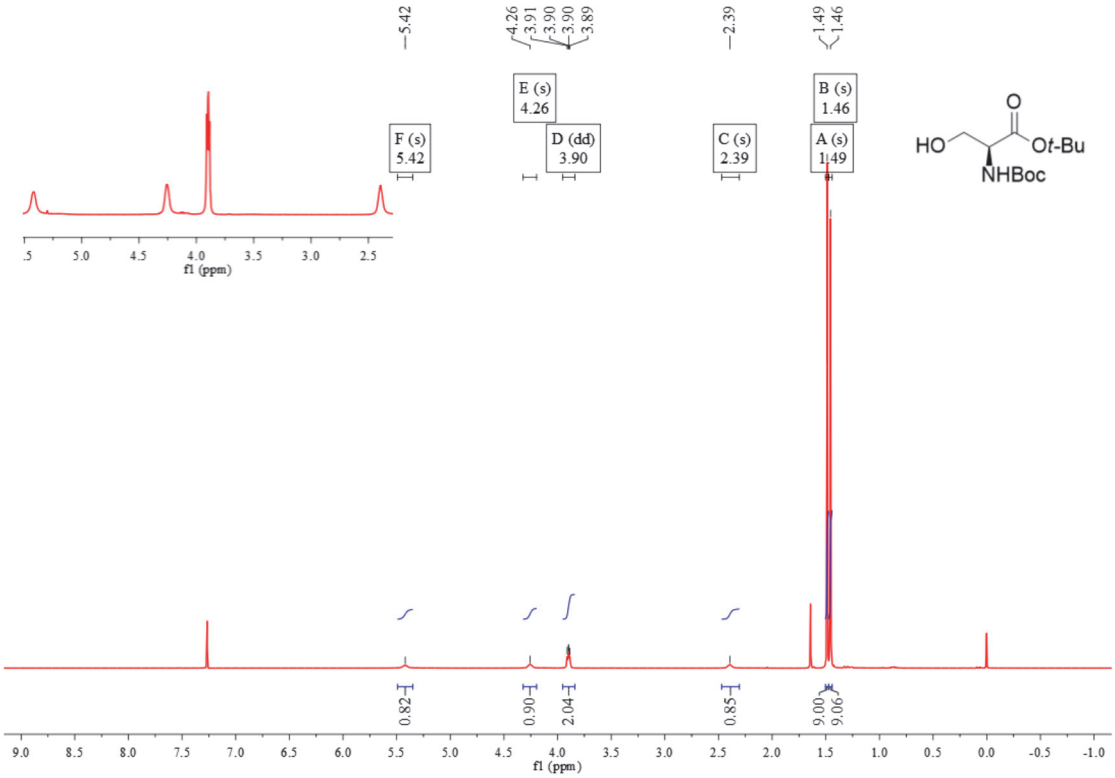
5.42
4.26
3.91
3.90
3.90
3.89
2.39
1.49
1.46
F (s) 5.42
E (s) 4.26
D (dd) 3.90
C (s) 2.39
B (s) 1.46
A (s) 1.49
HO
O
Ot-Bu
NHBoc
0.82
0.90
2.04
0.85
9.00
9.06
9.0 8.5 8.0 7.5 7.0 6.5 6.0 5.5 5.0 4.5 4.0 3.5 3.0 2.5 2.0 1.5 1.0 0.5 0.0 -0.5 -1.0
f1 (ppm)

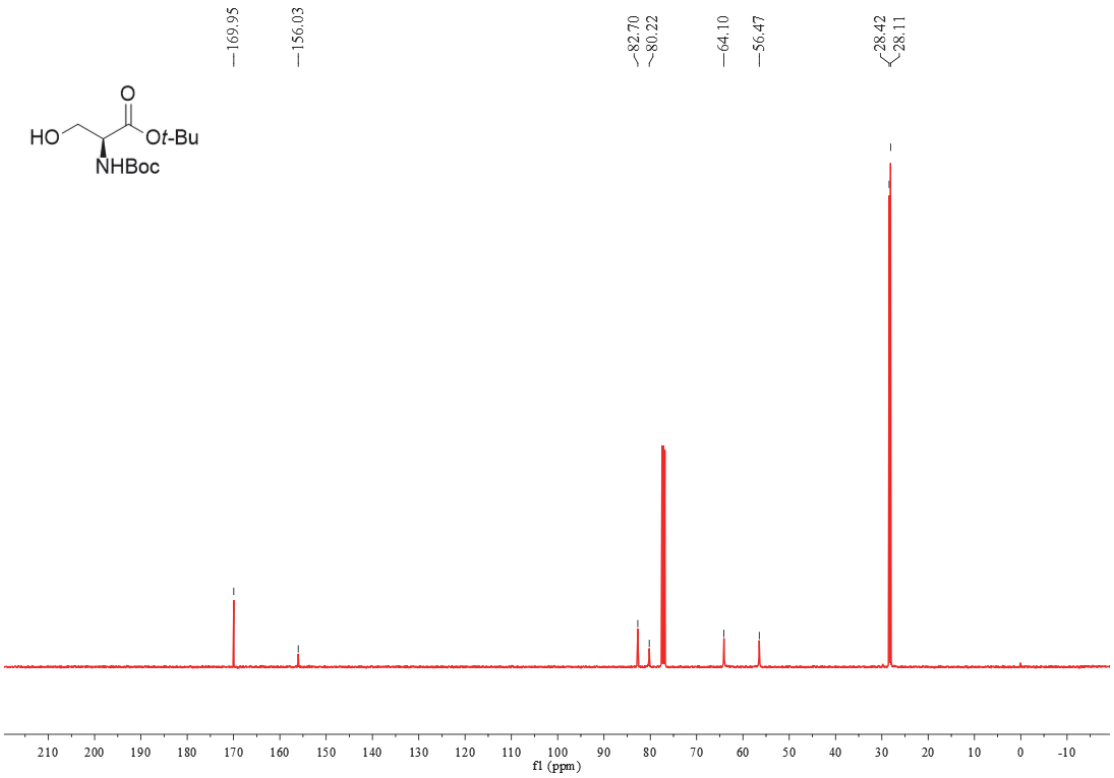
169.95
156.03
82.70
80.22
64.10
56.47
28.42
28.11
HO
O
Ot-Bu
NHBoc
f1 (ppm)

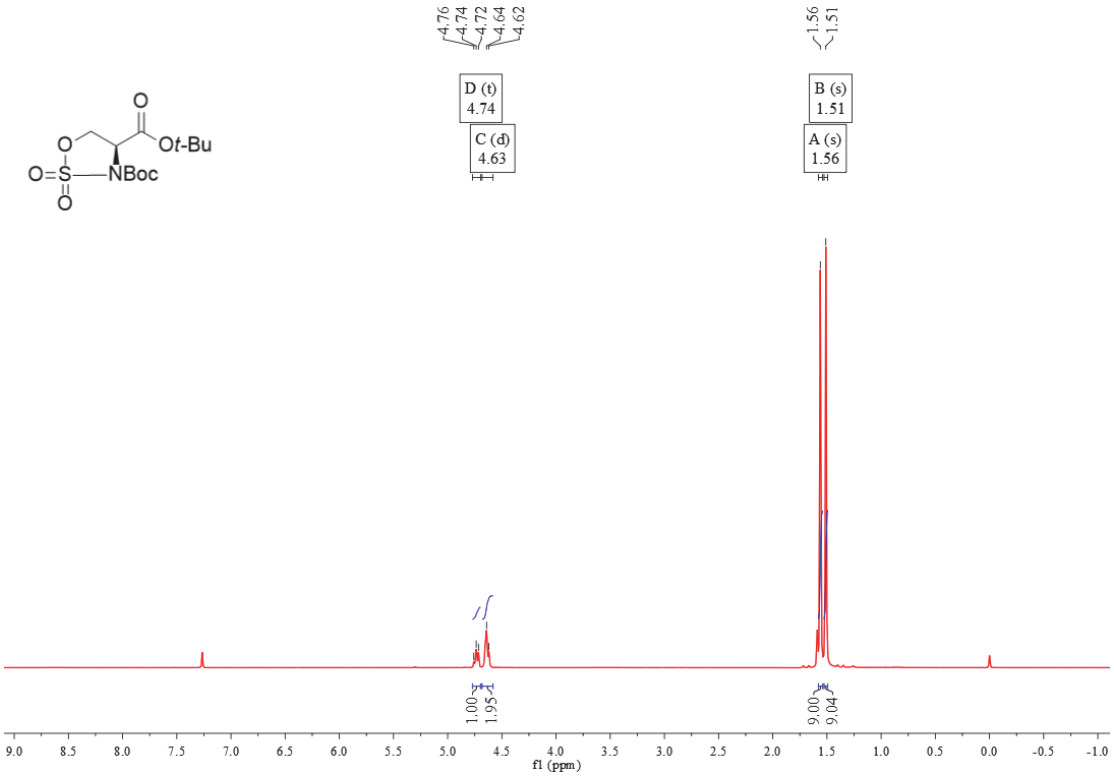
4.76
4.74
4.72
4.64
4.62
1.56
1.51
D (t)
4.74
C (d)
4.63
B (s)
1.51
A (s)
1.56
O
Ot-Bu
O=S
NBoc
1.00
1.95
9.00
9.04
f1 (ppm)

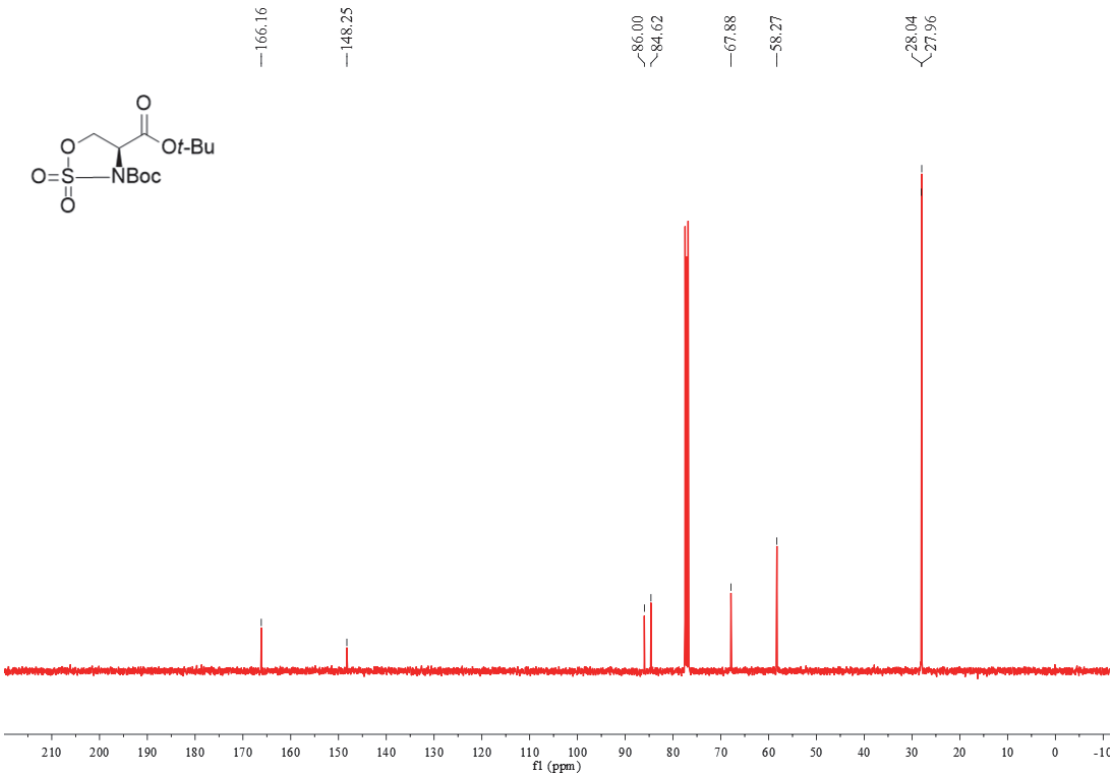
166.16
148.25
86.00
84.62
67.88
58.27
28.04
27.96
O
O
Ot-Bu
O=S
NBoc
O
210 200 190 180 170 160 150 140 130 120 110 100 90 80 70 60 50 40 30 20 10 0 -10
f1 (ppm)

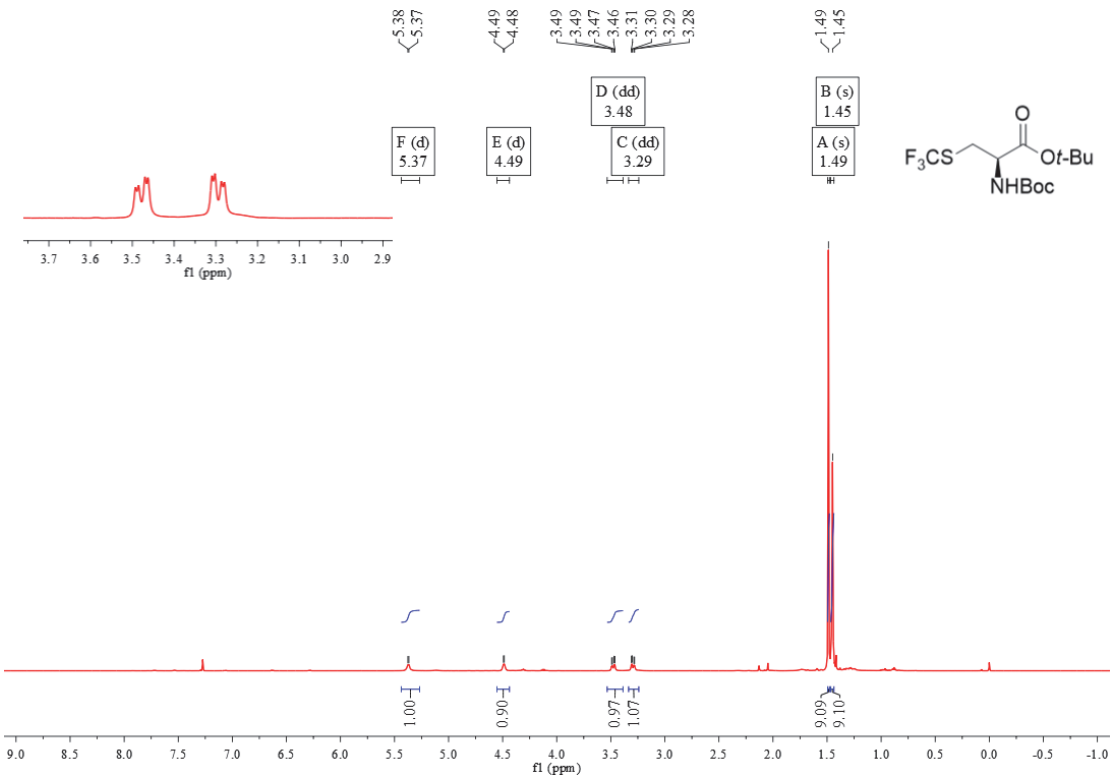
5.38
5.37
4.49
4.48
3.49
3.49
3.47
3.46
3.31
3.30
3.29
3.28
1.49
1.45
F (d)
5.37
E (d)
4.49
D (dd)
3.48
C (dd)
3.29
B (s)
1.45
A (s)
1.49
F3CS
Ot-Bu
NHBoc
3.7 3.6 3.5 3.4 3.3 3.2 3.1 3.0 2.9
f1 (ppm)
1.00
0.90
0.97
1.07
9.09
9.10
9.0 8.5 8.0 7.5 7.0 6.5 6.0 5.5 5.0 4.5 4.0 3.5 3.0 2.5 2.0 1.5 1.0 0.5 0.0 -0.5 -1.0
f1 (ppm)

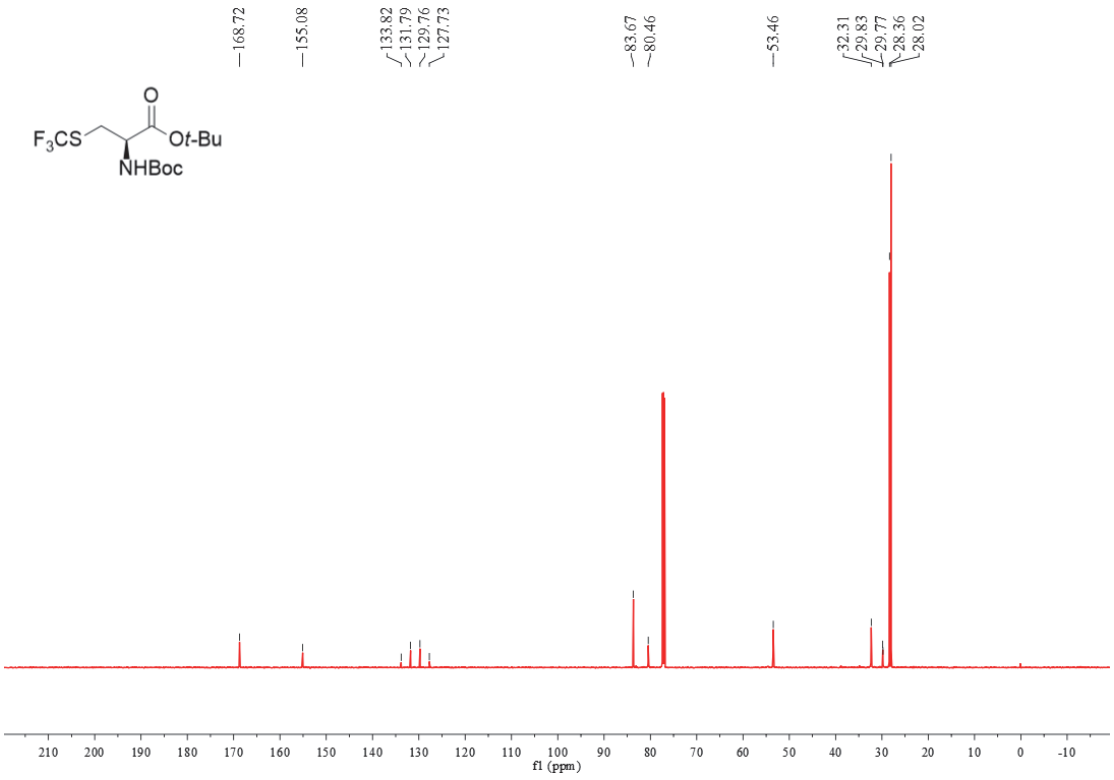
168.72
155.08
133.82
131.79
129.76
127.73
83.67
80.46
53.46
32.31
29.83
29.77
28.36
28.02
F3CS
O
Ot-Bu
NHBoc
f1 (ppm)

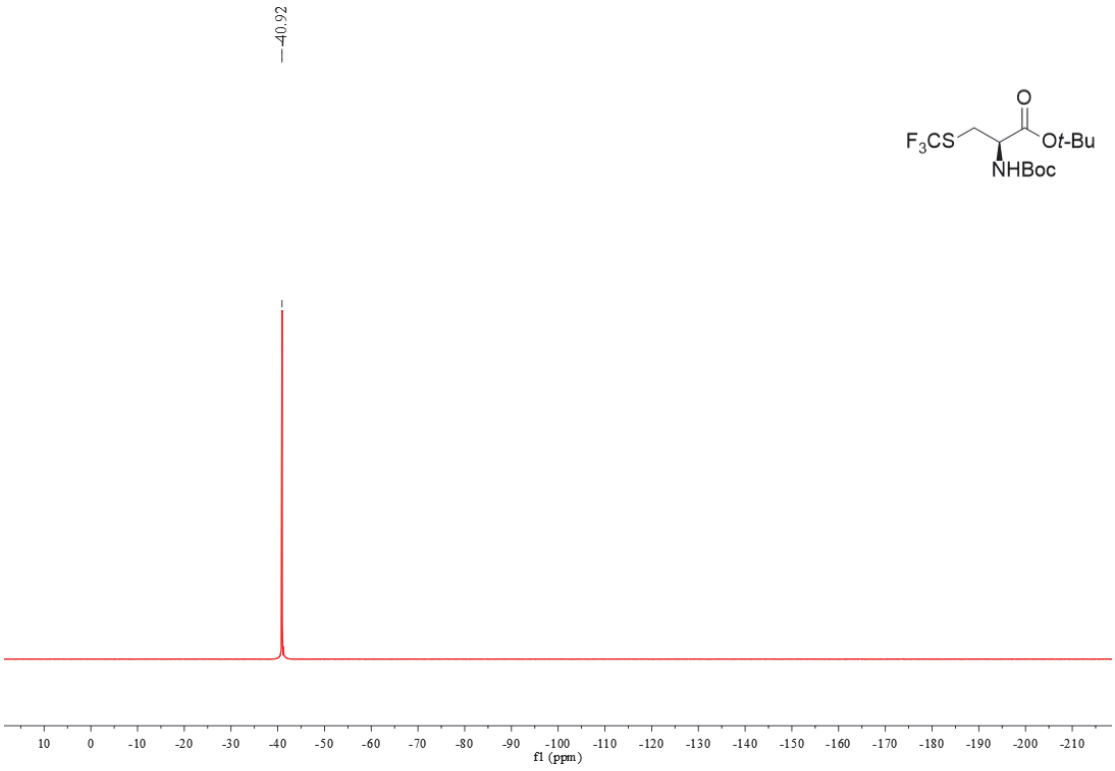
40.92
F3CS
O
Ot-Bu
NHBoc
f1 (ppm)

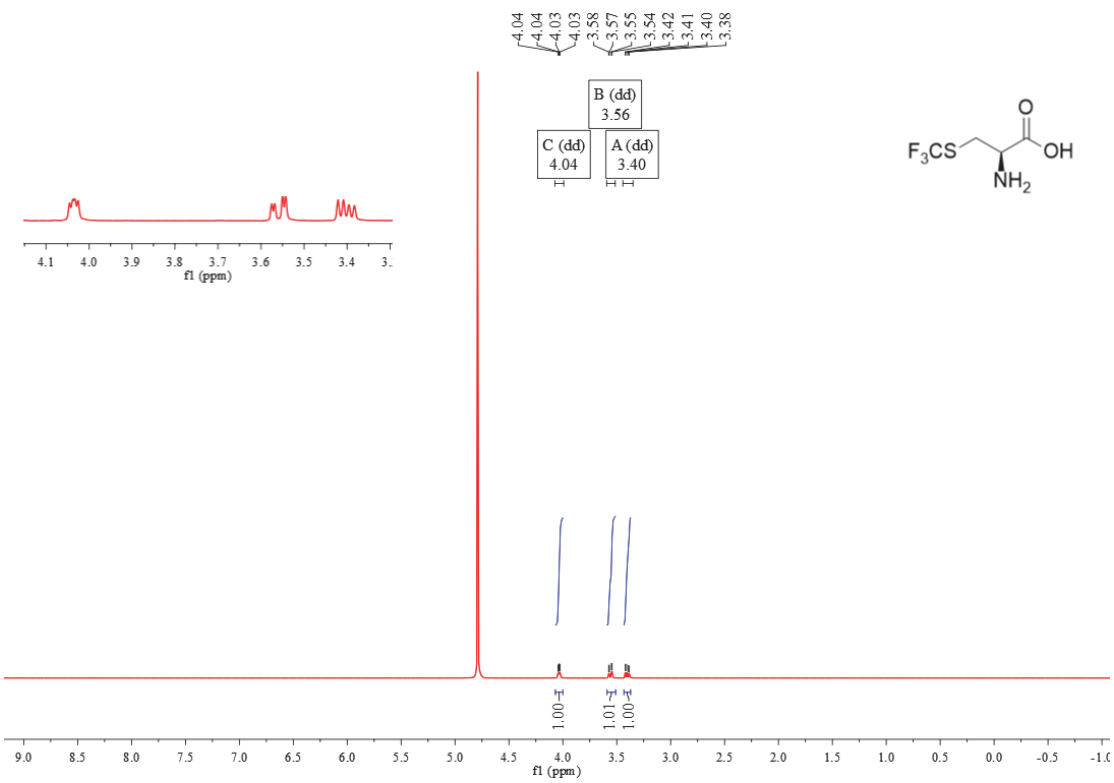
4.04
4.04
4.03
4.03
3.58
3.57
3.55
3.54
3.42
3.41
3.40
3.38
B (dd)
3.56
C (dd)
4.04
A (dd)
3.40
F3CS
OH
NH2
1.00
1.01
1.00
f1 (ppm)

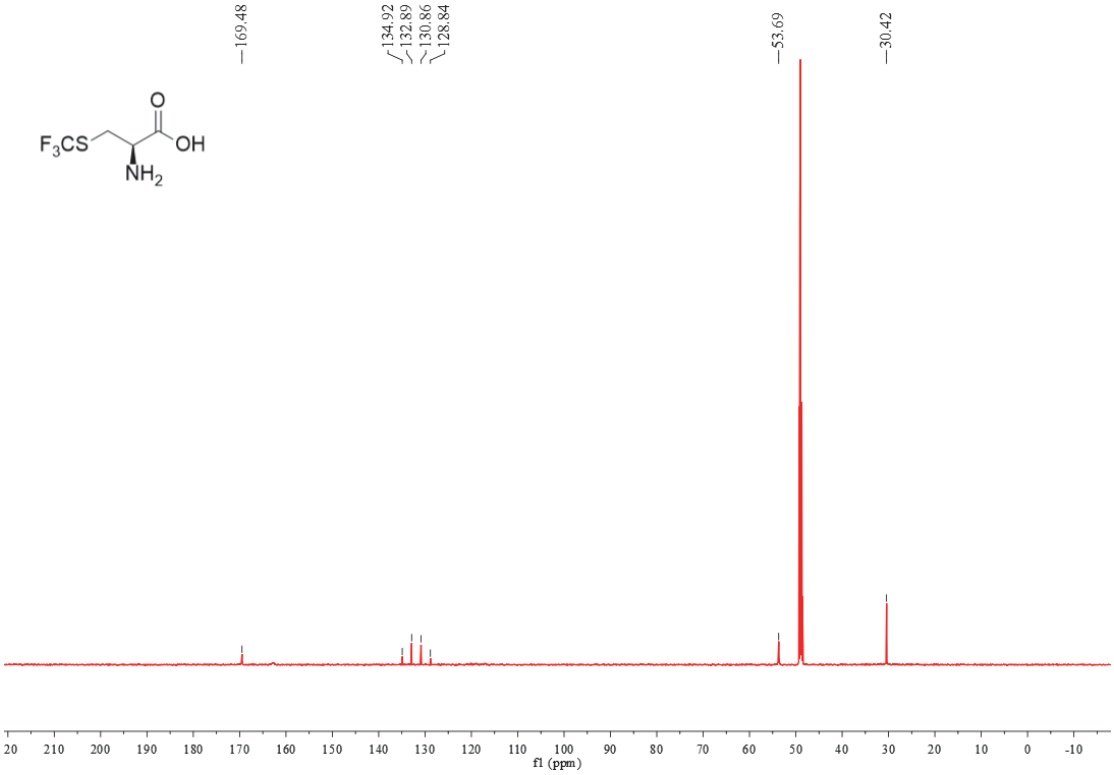
169.48
134.92
132.89
130.86
128.84
53.69
30.42
F3CS
OH
NH2
f1 (ppm)

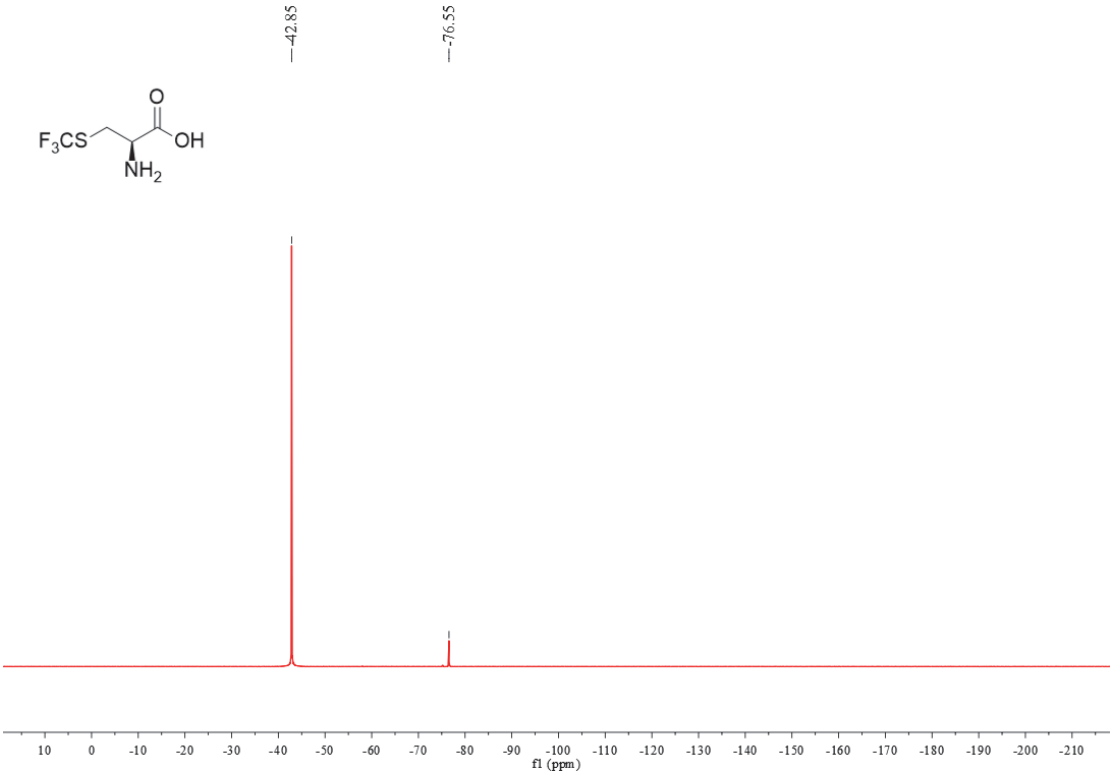
-42.85
-76.55
F3CS
O
OH
NH2
10 0 -10 -20 -30 -40 -50 -60 -70 -80 -90 -100 -110 -120 -130 -140 -150 -160 -170 -180 -190 -200 -210
f1 (ppm)

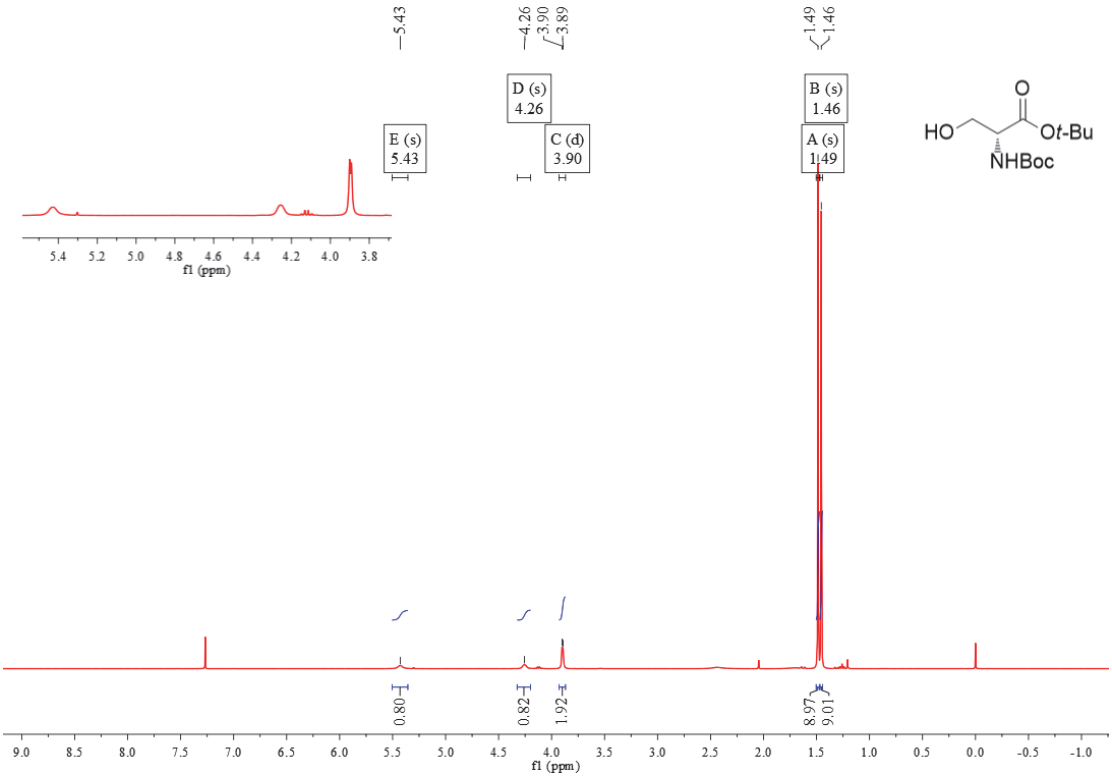
5.43
4.26
3.90
3.89
1.49
1.46
E (s) 5.43
D (s) 4.26
C (d) 3.90
B (s) 1.46
A (s) 1.49
HO
O
Ot-Bu
NHBoc
5.4 5.2 5.0 4.8 4.6 4.4 4.2 4.0 3.8
f1 (ppm)
0.80
0.82
1.92
8.97
9.01
9.0 8.5 8.0 7.5 7.0 6.5 6.0 5.5 5.0 4.5 4.0 3.5 3.0 2.5 2.0 1.5 1.0 0.5 0.0 -0.5 -1.0
f1 (ppm)

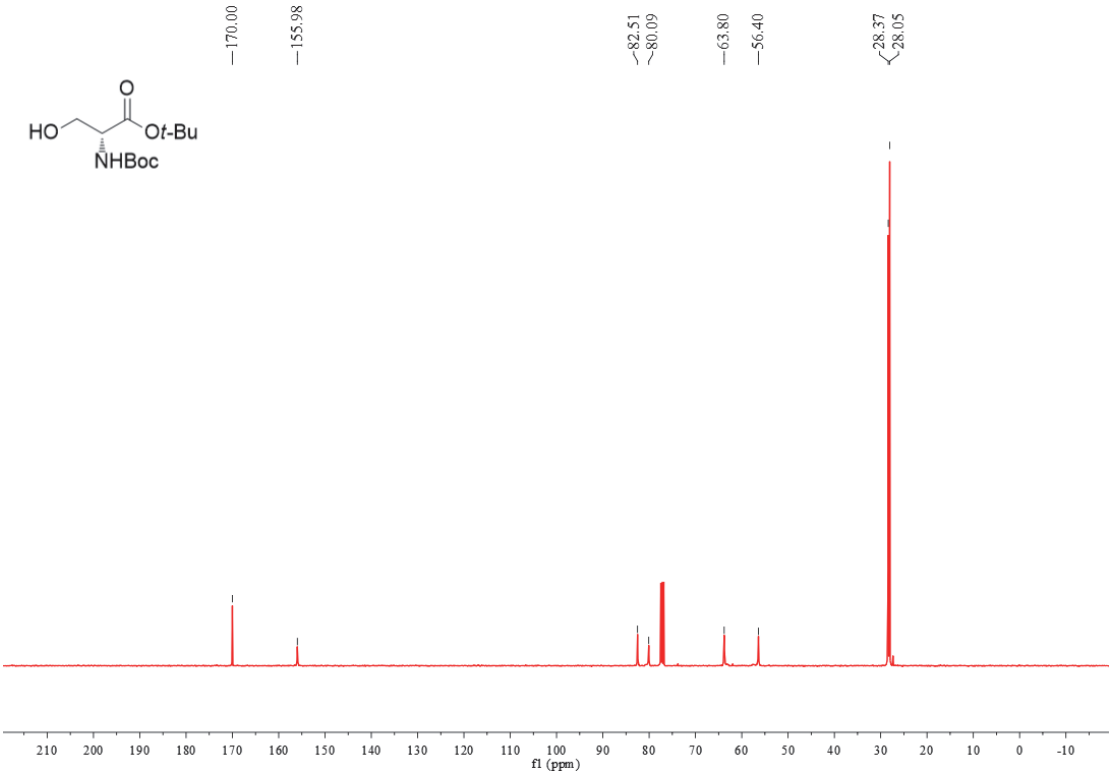
170.00
155.98
82.51
80.09
63.80
56.40
28.37
28.05
HO
O
Ot-Bu
NHBoc
f1 (ppm)

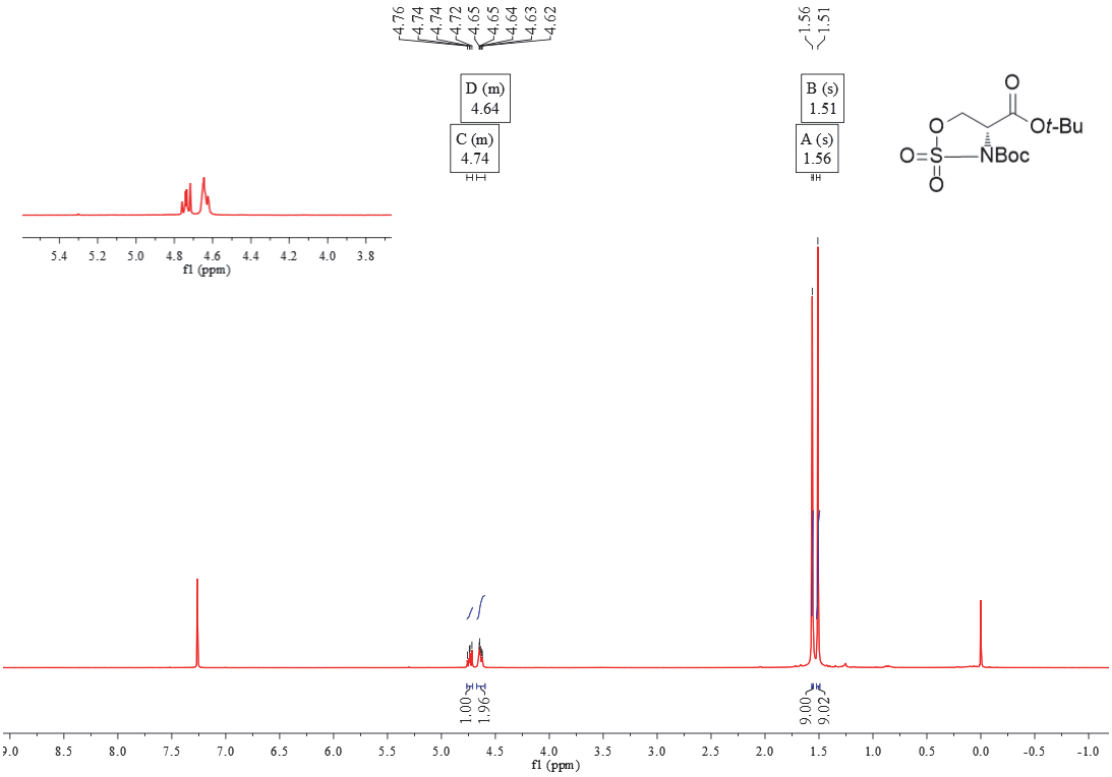
4.76
4.74
4.74
4.72
4.65
4.65
4.64
4.63
4.62
1.56
1.51
D (m)
4.64
C (m)
4.74
B (s)
1.51
A (s)
1.56
O
Ot-Bu
O=S
NBoc
O
1.00
1.96
9.00
9.02
f1 (ppm)

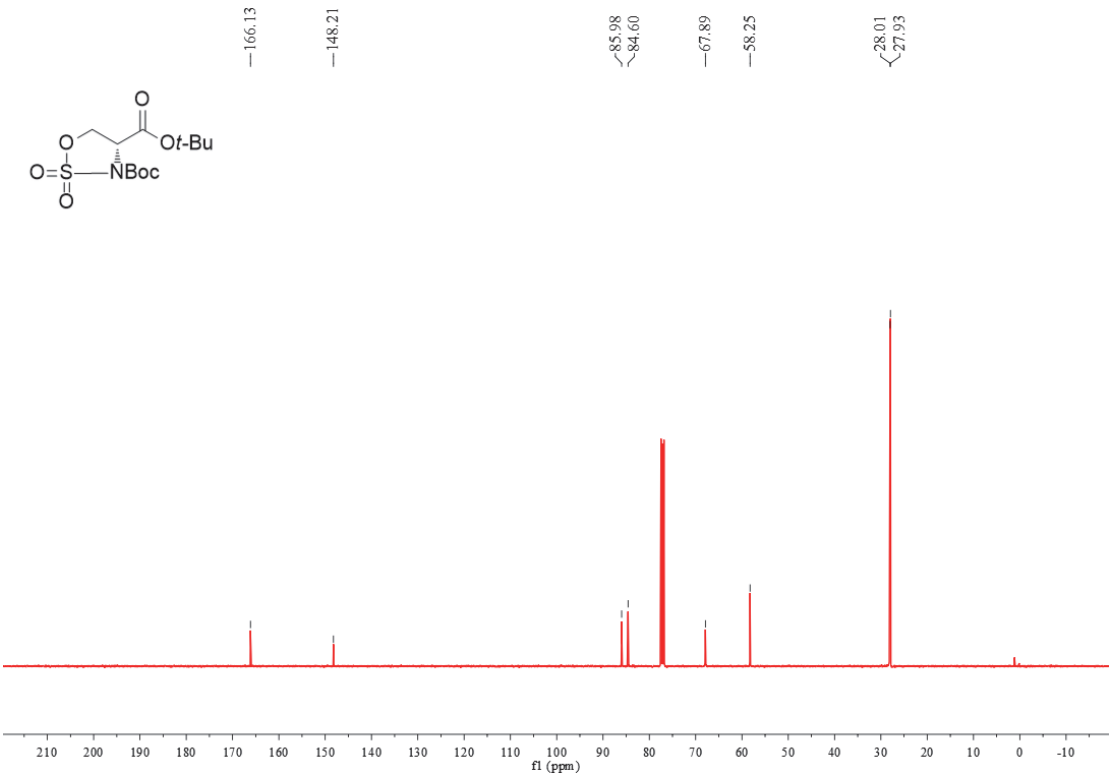
166.13
148.21
85.98
84.60
67.89
58.25
28.01
27.93
O
O
Ot-Bu
O=S
NBoc
O
210 200 190 180 170 160 150 140 130 120 110 100 90 80 70 60 50 40 30 20 10 0 -10
f1 (ppm)

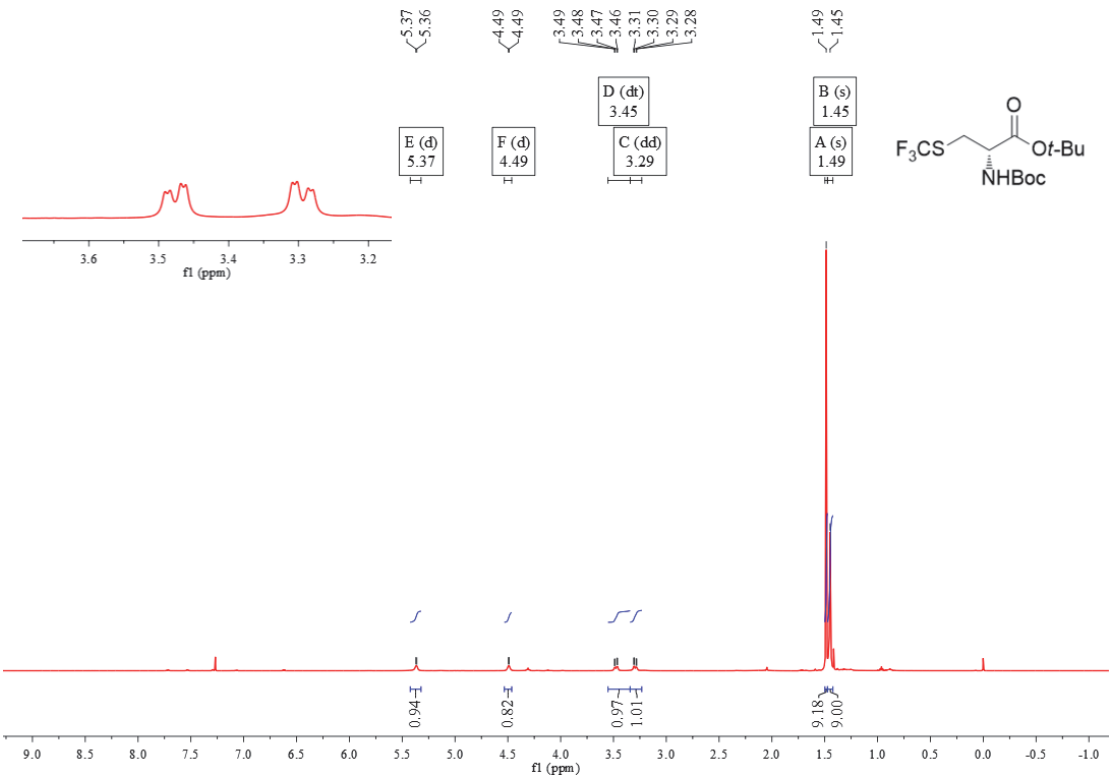
5.37
5.36
4.49
4.49
3.49
3.48
3.47
3.46
3.31
3.30
3.29
3.28
1.49
1.45
D (dt)
3.45
B (s)
1.45
E (d)
5.37
F (d)
4.49
C (dd)
3.29
A (s)
1.49
F3CS
O
Ot-Bu
NHBoc
3.6 3.5 3.4 3.3 3.2
f1 (ppm)
0.94
0.82
0.97
1.01
9.18
9.00
9.0 8.5 8.0 7.5 7.0 6.5 6.0 5.5 5.0 4.5 4.0 3.5 3.0 2.5 2.0 1.5 1.0 0.5 0.0 -0.5 -1.0
f1 (ppm)

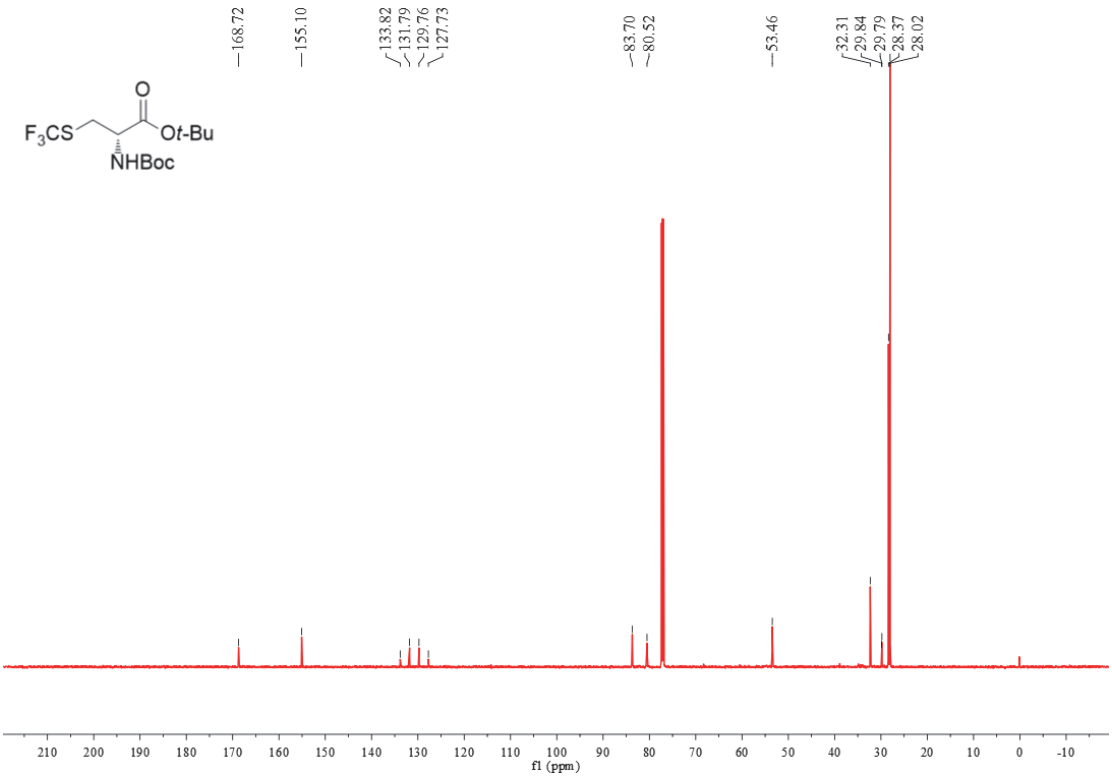
168.72
155.10
133.82
131.79
129.76
127.73
83.70
80.52
53.46
32.31
29.84
29.79
28.37
28.02
F3CS
O
Ot-Bu
NHBoc
f1 (ppm)

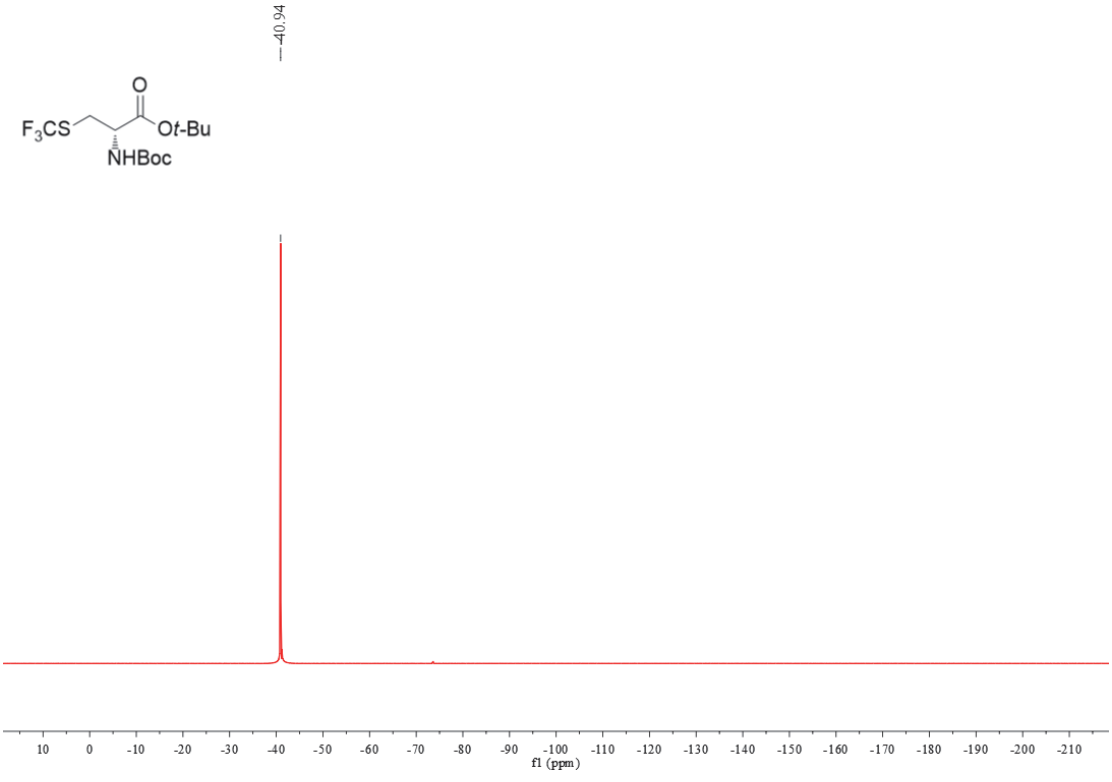
40.94
F3CS
O
Ot-Bu
NHBoc
f1 (ppm)

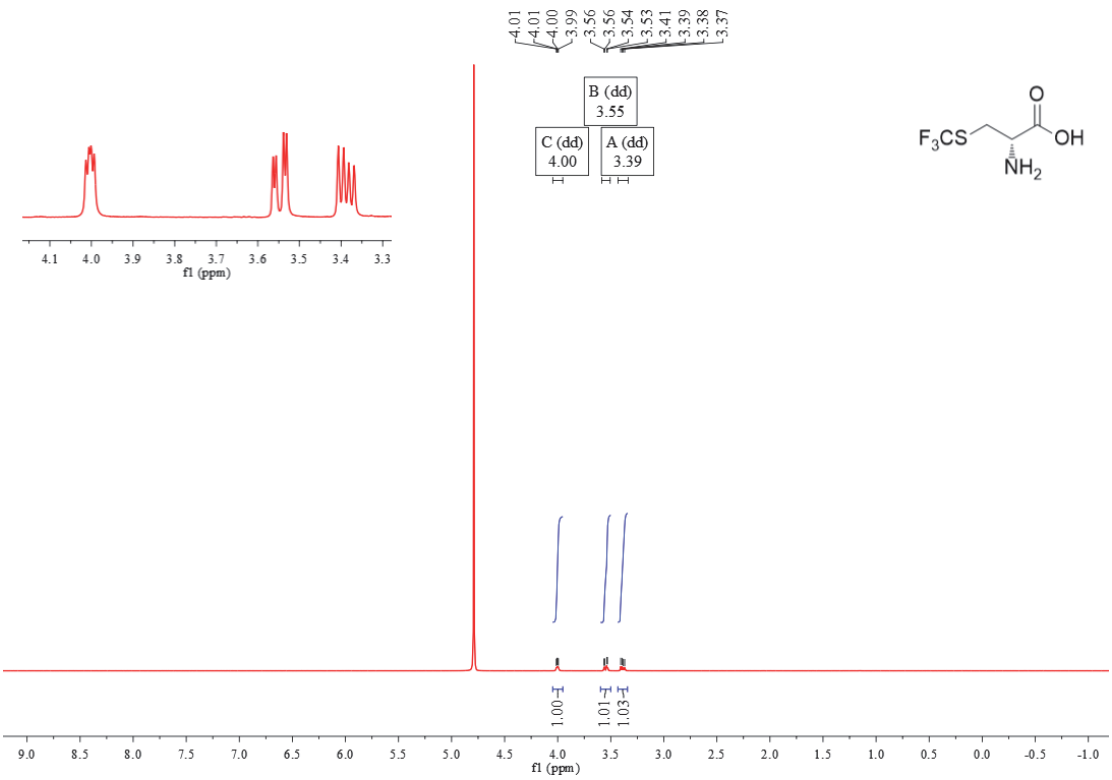
4.01
4.01
4.00
3.99
3.56
3.56
3.54
3.53
3.41
3.39
3.38
3.37
B (dd)
3.55
C (dd)
4.00
A (dd)
3.39
F3CS
OH
NH2
f1 (ppm)
1.00
1.01
1.03

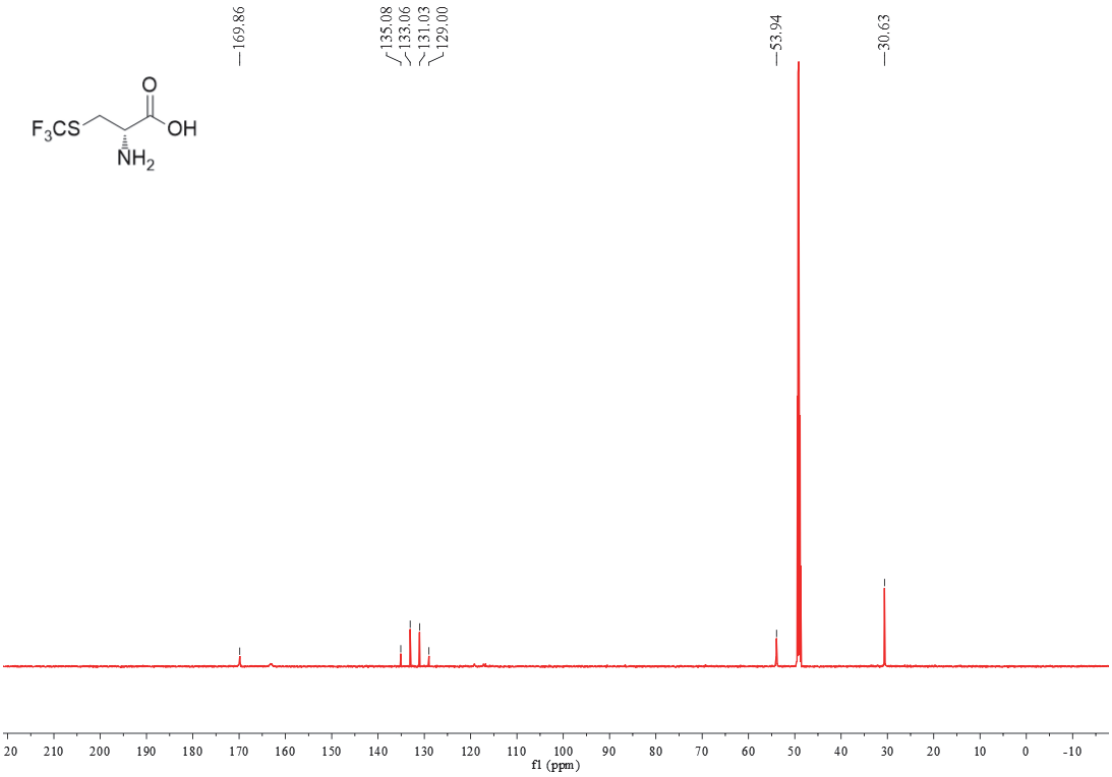
169.86
135.08
133.06
131.03
129.00
53.94
30.63
F3CS
OH
NH2
f1 (ppm)

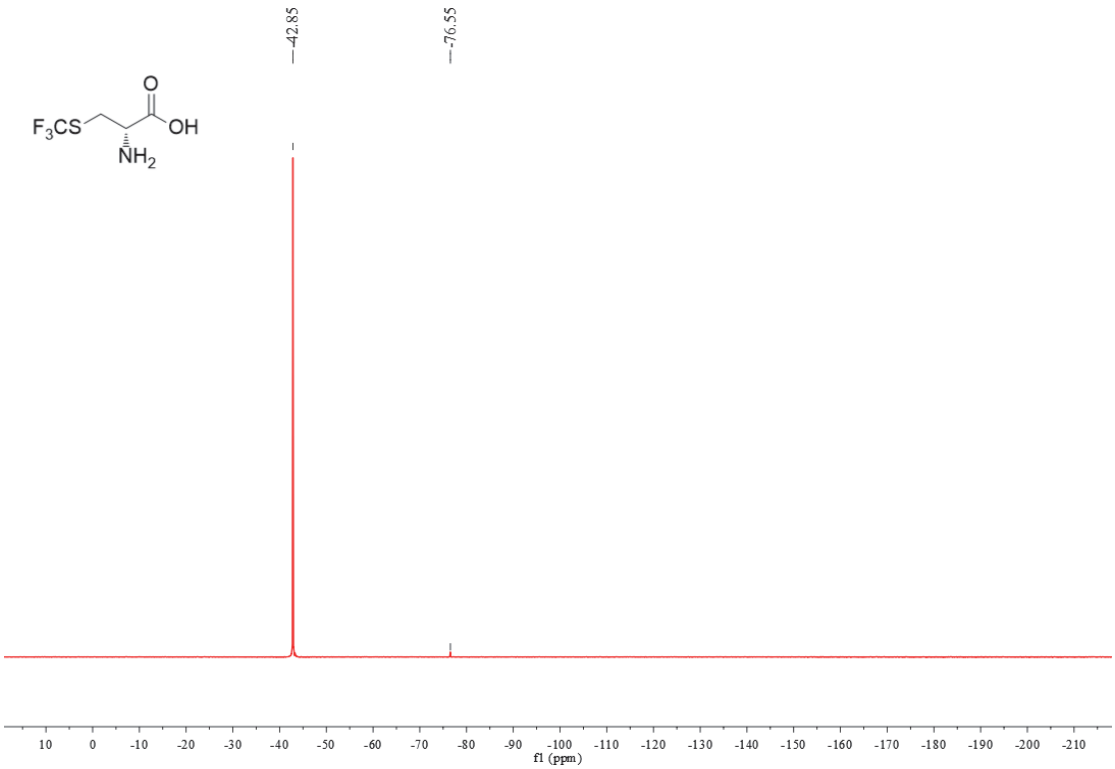
-42.85
-76.55
F3CS
O
OH
NH2
10 0 -10 -20 -30 -40 -50 -60 -70 -80 -90 -100 -110 -120 -130 -140 -150 -160 -170 -180 -190 -200 -210
f1 (ppm)